Sub Rosa
Monitoring LLC

Liberty Star Minerals

Redrock Canyon
IP and Resistivity
Field Survey
July 24-30, 2025

Date Submitted: October 16, 2025

This report summarizes the IP and resistivity data collected in July 2025 at Liberty Star's Redrock Canyon Project near Tombstone Arizona.

Table of Contents

Executive Summary 3
Survey Location 5
Data Collection and Processing 6
Plan map of near surface data 7
Data Discussion 9
Line 1 Data 10
Deep Response 11
Line 2 Data 11
Line 3 Data 13
Line 4 Data 15
Line 5 Data 17
3D Data 18
Three-dimensional Inversions 18
ResMod3DInv Resistivity Image 19
ERTlab64 Resistivity Image 20
ResMod3DInv IP Image 21
Recommendations 21
References 23
APPENDIX A 24
Data statistics 24
Vein Signature Discussion 26
Inversion Modeling 34
Line 1 Inverted Sections 35
Line 2 Inverted Sections 36
Line 3 Inverted Sections 37
Line 4 Inverted Sections 38
Line 5 Inverted Sections 39

Figure 1: Inverted resistivity volume 4
Figure 2: 3D view of inverted IP data 4
Figure 3: Google Earth image of survey location. 6
Figure 4: Plan maps of the surface resistivity and chargeability 8
Figure 5: Line 1 Apparent Resistivity and IP raw data pseudosections 10
Figure 6: Line 2 Apparent Resistivity and IP raw data pseudosections 12
Figure 7: Line 3 Apparent Resistivity and IP raw data pseudosections.. 14
Figure 8: Line 4 Apparent Resistivity and IP raw data pseudosections 16
Figure 9: Line 5 Apparent Resistivity and IP raw data pseudosections 17
Figure 10: Redrock Canyon ResMod3DInv 3D resistivity image. 19
Figure 11: Redrock Canyon 3D ERT*lab*64 resistivity image. 20
Figure 12: Redrock Canyon ResMod3DInv 3D IP image. 21

Liberty Star Redrock Canyon IP Survey

Executive Summary

During the period July 24th through 30th, 2025 Sub Rosa Monitoring LLC performed a resistivity and induced polarization (IP) survey over a small grid within the Redrock Canyon site located approximately 5 miles southeast of Tombstone, Arizona. The survey was conducted over an area previously tested with drilling. The primary purpose of the survey was to determine the correlation, if any, between the areas of known gold mineralization and the electrical geophysics.

Survey results were compared to drillholes with assay data. A good correlation between both resistivity and IP with the jasperoidal veining, associated sulfides and gold assays in the drillholes was confirmed. Throughout the survey the detected physical property contrasts between the hosting limestone and jasperoidal veins were relatively low but coherent and statistically mappable. The veins produced diagnostic signatures that were readily traceable to specific locations. The combination of mineralized veins and diffuse mineralization within the adjacent limestones provided easily identifiable drilling targets. The results of the survey provide confirmation that the known gold mineralization, previously determined from geochemistry and drilling, was readily manifested in the geophysical data. Structural features, either mineralized or not, and their orientations were detected and mapped by the electrical geophysics.

One of the challeges of the broader area is the thin veneer of soil covering many of the veins that could, and perhaps should, be sampled. This survey has demonstrated that those covered veins can be readily detected, mapped and categorized for future sampling and drilling.

The resolution of the geophysics is shown in two examples. A three dimensional view of inverted resistivity data with relevant drillholes is presented in Figure 1. The green isosurface encloses resistivities greater than 10,500 ohm-meters and encompasses the area of most intense veining. The view is looking easterly. Drillhole gold assays are scaled by value; red is the highest of these holes at 15 ppm.

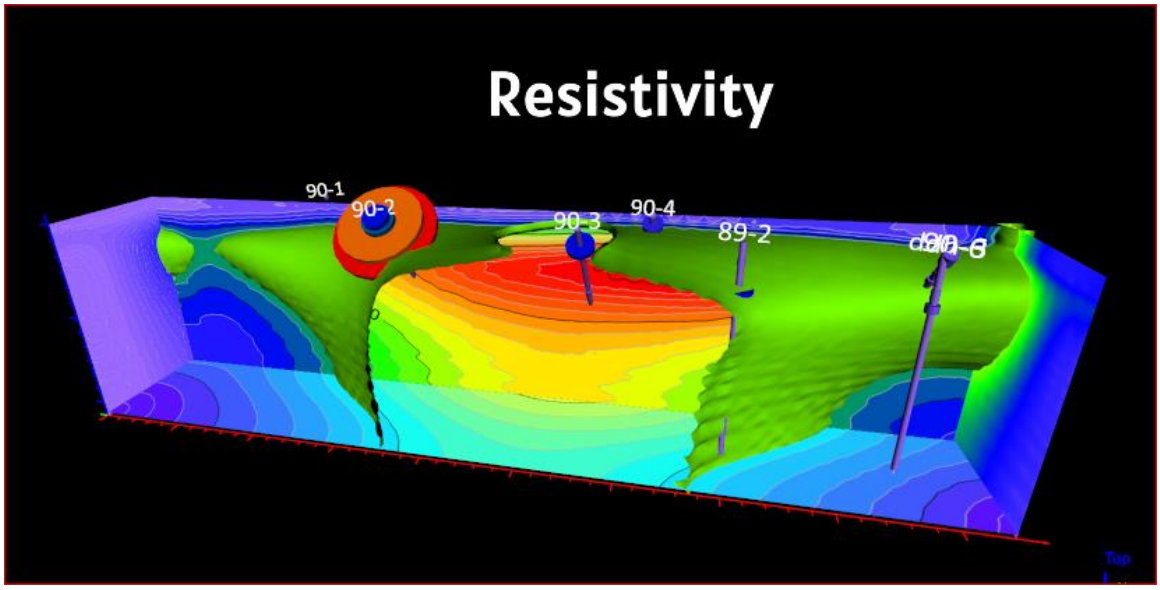

Figure 1: Inverted resistivity volume
This image shows an isosurface of 10,500 ohm-meters, relevant drillholes, and related gold assays.

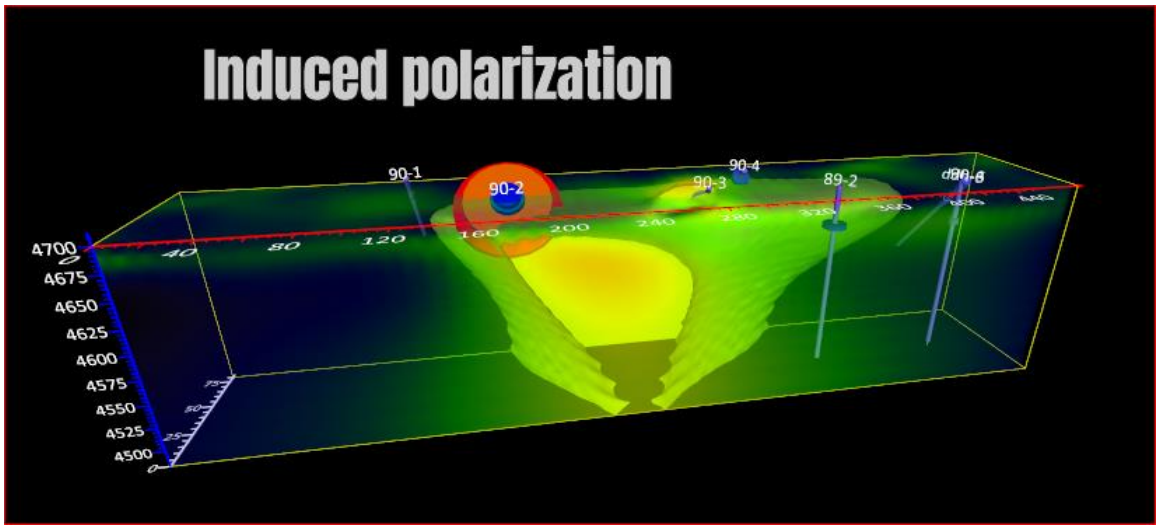

Figure 2: 3D view of inverted IP data
This image shows an isosurface of 14mV/V and drillholes located within the survey grid. View is looking easterly.

Figure 2 displays a similar isosurface of the IP data enclosing the volume of higher chargeabilities. The extension to depth in both examples is questionable and may result from the masking effect of the extensive veining at surface.

Survey Location

The survey was located about 5 miles southeast of Tombstone, Cochise County, Arizona in the northwest quarter of the southwest quarter of Section 28, Township 26 South, Range 23 East, Gila and Salt River Meridian. The survey grid was 470 feet long in the north-south direction and 80 feet wide. It consisted of five north-south lines spaced 20 feet apart. Electrode spacing was 10 feet. It was so placed to encompass some of the existing drillholes. One of the primary purposes of the IP survey was to determine the relationship between IP response and gold-containing-sulfides. This area had been drilled and the presence of gold and sulfides confirmed. It offered the possibility of being a nearly ideal "calibration" site and was chosen as the preferred location for the IP survey. Figure 3 shows the grid and drillholes on a Google Earth image. With some brush clearing, vehicular access was enabled to the center of the grid. The general area has also been targeted by rock-chip and trench sampling geochemistry so is well studied and a good calibration site. This particular area has been the most intensely studied area within the Redrock Canyon/Hay Mountain general area and a good deal of information is available in previous reports.

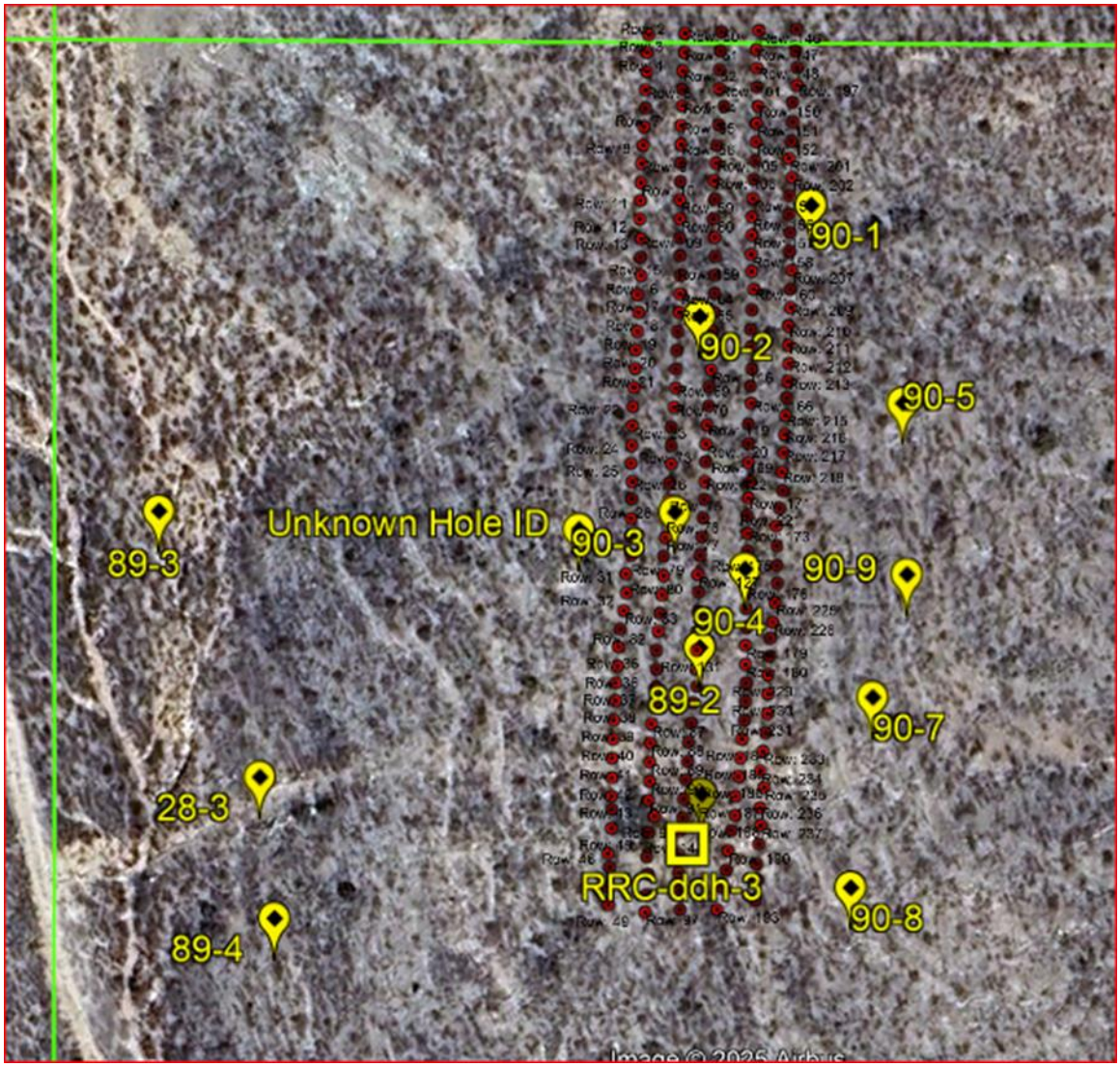

Figure 3: Google Earth image of survey location.
The survey grid are red dots and drillholes are yellow symbols. The green lines are the north and west boundaries of the northwest quarter (40 acres) of the southwest quarter (160 acres) of Section 28, T26S R23E.

Data Collection and Processing

The resistivity and IP data were acquired between July 24 and 30, 2025. The Figure above shows the data collection lines and the locations of each electrode. The survey consisted of five lines oriented roughly north-south using a pole-pole array with interelectrode spacings ranging from 10 to 470 feet. The lines were roughly parallel and placed approximately 20 feet apart forming a grid to allow three-dimensional inversion.

The north/south lines are referred to as Lines 1 through 5, with Line 1 being the western most line. Electrode stations are numbered 1 through 470 from north to south. After

installing the electrodes, in a few cases in holes drilled into the outcropping limestone, each line was tested to ensure adequate electrode response. Electrodes were stainless steel rods 18" long. The data acquisition system was a battery-powered Multi-Phase Technologies, LLC. Digital Acquisition System (DAS-1). The instrument was located within the grid in an air-conditioned trailer. All electrodes were connected to the DAS via multi-conductor cables and jumper wires. Remote electrodes were placed approximately 1,800 feet to the east for the remote receiver (potential) electrode and approximately 2,600 feet to the south for the remote transmitter electrode. Their influence was compensated for during data processing. Total electrode count was 240 creating a grid 470 feet long (north-south) by 80 feet wide (east-west). Apparent resistivities ranged from high hundreds of ohm-meters to several thousand ohm-meters, typical for operations on such shallow bedrock.

Electrode locations were determined by survey-grade GPS (Ashtech MobileMapper) capable of using both GPS (USA) and GLONASS (Russia) satellites enhanced by an external antenna (Ashtech 111660). Horizontal and vertical accuracy is within ±½ foot.

Resistivity and IP data were acquired in the time-domain mode (TDIP) using a 0.125 Hz, 50% duty cycle square wave (2 sec on, 2 sec off, 2 sec reversed polarity, 2 sec off). Resistivity data were calculated in ohm-meters. IP data are the average of three consecutive windows observed starting at 10 milliseconds after current cessation. IP values are reported in millivolts per volt (mV/V). Transmitted currents ranged from 10 to 300 milliamps which, combined with the pole-pole configuration, provided high signal-to-noise ratios. Telluric signals and random noise were negligible. Waveforms were stacked for 8 and 10 periods resulting in high quality data. No data had to be rejected due to noise.

Field operations were overseen by Liberty Star's V. P. of Field Operations, Mr. Jay Crawford. Sub Rosa field staff were Dr. J. B. Fink, C.T.O., Dr. Gail L. Heath, C.O.O., and Michael Royan, C.E.O.

Plan map of near surface data

One of the simplest ways to view the resultant data and how they compare with, or relate to, the surface geology is to focus on the shallowest data. In this case, that information comes from the shortest electrode spacings which were nominally 10 feet apart and the lines, 20 feet apart. Contouring these data generates a map of the electrical properties of the surface and a few feet into the ground. Maps of the shallowest resistivity and chargeability data are shown in Figure 4.

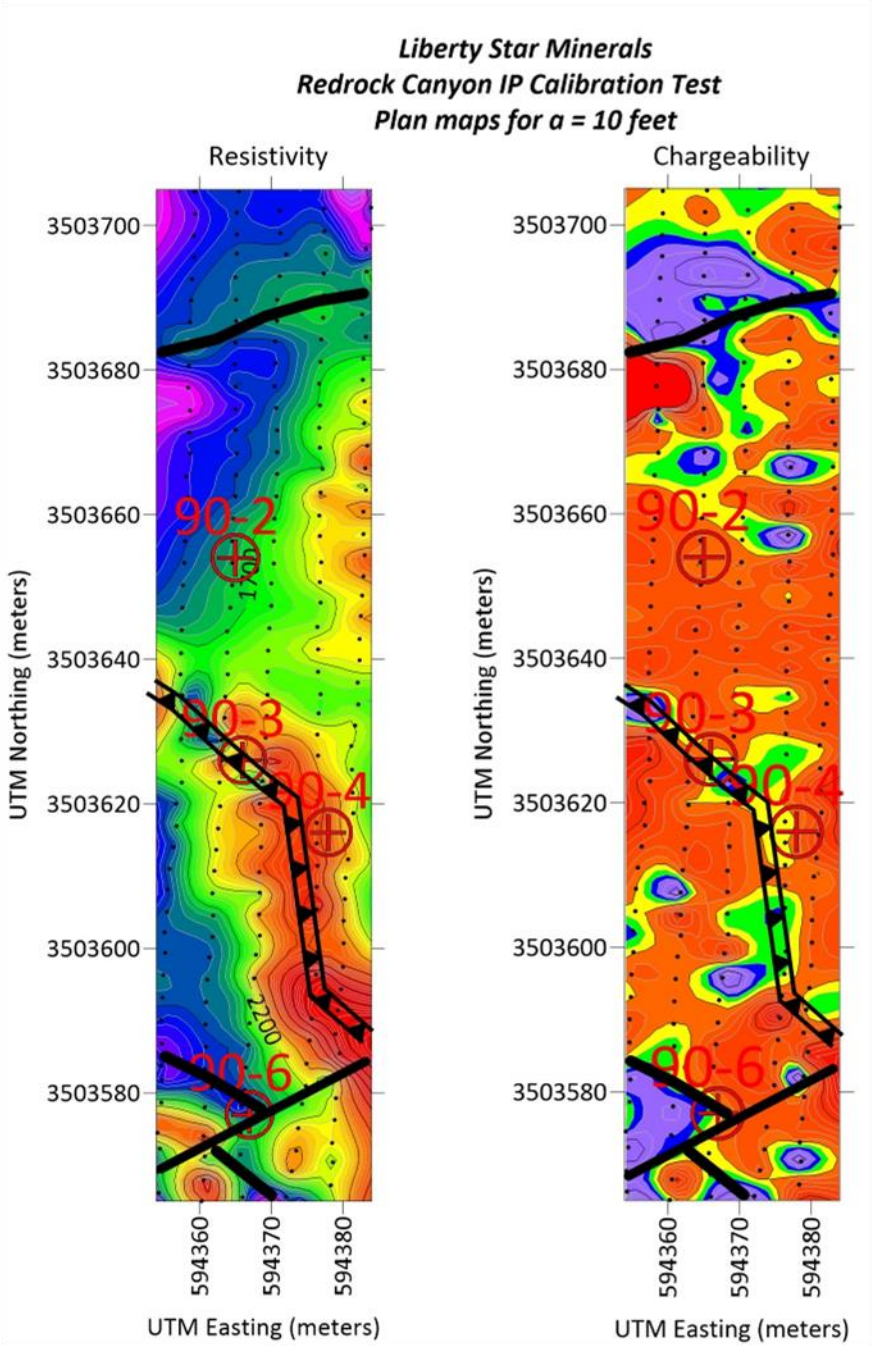

Figure 4: Plan maps of the surface resistivity and chargeability
The image represents values acquired at the shortest electrode spacing of 10 feet. Halterman's feeder structure is the double hatched line, other lines are interpreted structures.

The warm colors are higher resistivities and chargeabilities and the cooler colors indicate lower values of both. The higher resistivities are most evident in the southern and eastern portions of the grid. They represent extensive veining and stringers associated with jasperoid and siliceous breccia exposed at, and near, surface. In particular, the highest resistivities are also associated with confirmed gold mineralization. In contrast, the cooler colors in the northwestern and northern areas reflect increasing thickness of the alluvial

cover. Later discussions will reveal some surprising results in this area as well. The chargeability data are uniformly elevated within the structural bounds but do not show a strong correlation with the veining represented in the resistivity data.

Data Discussion

Previous surveys (over much of the Hay Mountain project area) have encountered resistivities associated with the limestones in the thousands of ohm-meters (Fink, 2021). Because the present survey was entirely placed in an area of extensive outcropping limestone we anticipated even higher resistivities perhaps in excess of 10,000 ohm-meters. Grouping all five lines and looking at the statistics, we don't really see that. We have 5,384 data points with an average of 2,400 ohm-meters. We infer from the apparent resistivity data that the area covered by the survey has increased porosity and permeability possibly due to the known mineralization and structural breakup, as compared to predicted resistivities for unaltered limestone in the high thousands (Parkhomenko, 1967). The maximum observed resistivity was 5,700 ohm-meters and the minimum was 600 ohm-meters. More detailed statistics and histograms are presented in Appendix A.

In addition to performing computer inversions, we support presenting, discussing and interpreting the raw data which are used in the inversions. This is of particular importance at this location due to the mineralized veining. The raw data clearly isolate individual veins but the inversion software instead produces a blended result.

The following discussion on a line-by-line basis requires some preparatory comments. The data are presented in two side-view pseudosections of apparent resistivity and induced polarization. This approach displays the raw data in sectional form using a logarithmic vertical compression of the data point locations. A logarithmic vertical distribution reflects the manner in which the depth-of-investigation varies with expanding electrode spacing. Additionally the data point locations are "hung" on topography which in our case is very nearly flat and has minimal influence. The key point is that regardless of how the data are presented they are in no way altered from the actual values. This is important because in dealing with dikes and veins, as explained above, we encounter unusual artifacts that all too frequently get lost in editing and filtering data for inversion. The present data set, in toto, has numerous dike-like responses that are extremely important to understanding the geologic structure of the target area and, in fact, pose a challenge for inversion.

When dike-like features occur near or at surface they tend to produce what are called "pant-leg" effects (in raw data) where the data create a pair of down-going ridges of high (or low) responses that look like pant-legs with intervening intermediate values. The character of these pant-leg responses can sometimes immediately reveal the physical properties of the dike-like feature, as well as a reasonably accurate location, as is seen in the present data set.

Line 1 Data

Figure 7 displays the Line 1 Apparent Resistivity and Induced Polarization in logarithmic pseudosection. View is looking east. Warm colors are higher values; cool colors are lower values. Salient features are indicated by arrows.

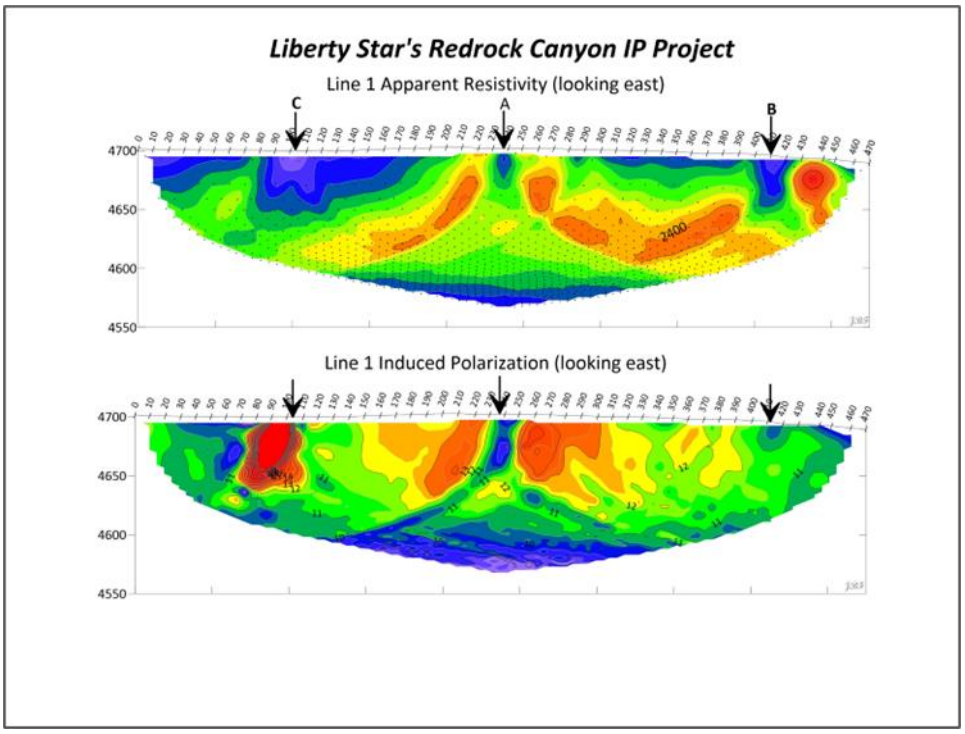

Figure 5: Line 1 Apparent Resistivity and IP raw data pseudosections
This psuedosection is hung on topography, looking east. See text for discussion.

The Line 1 apparent resistivity data display three striking features that represent mineralized vein structures. Features A and B are interpreted as steeply dipping, resistive, polarizable vein structures labeled on the resistivity section. They illustrate the vein signature discussed more extensively in Appendix A.

Feature A in the middle of the section near Station 240 is considered to represent Halterman's (1988, 1981) "feeder structure" and is a textbook example of a vein response. It is further manifested by a consistent response character on Lines 2 through 3 where it strikes roughly N45W-S45E in agreement with Halterman. However, after Line 3 we interpret it to be offset to the south by approximately 120 feet (~40 m) on and along Line 4 (as shown in Figure 4). The higher resistivities along Line 4 may represent the offset. Then, on Lines 4 and 5, this feature strikes again very roughly the same as the northwestern limb. Note that the IP response at surface is much broader than the high resistivity data and encompasses the trench gold grade of 167.5 ppm (sum over 2.4 ft). This broader response is reflected in the inversion results. Overall, this structure appears to coincide with and support Halterman's "feeder structure". Halterman reports an approximate strike of N40W and vertical dip; close enough. Halterman (1991) later states "*Silicification associated with this structure has been sampled and mapped. Samples have varied from trace to 1.02*

ounces per ton gold. Samples in excess of 0.1 ounce per ton gold are common." We adopt Halterman's "feeder structure" as the predominant feature in this IP survey.

Feature B at the south end of all the lines is where two drillholes have been placed; 90-6 and RCC ddh-3. It is a structurally more complex environment as indicated in Figure 4. Geochemical trench sample #12 immediately adjacent to the drillholes reported a total of 17.268 ppm gold over a 7 foot (2 m) trench almost entirely in jasperoidal breccia. This further illustrates the ability of IP and resistivity to target mineralized features in this environment.

Feature C happens to be the highest IP response of the entire survey. It occurs near Station 100 in the northwestern corner on Line 1. This feature is another vein-like response but may be over ten feet thick. The IP response is three-times background. It appears to project almost due east onto Line 2 but there it lacks the very high response and becomes a moderate-to-weak response. This feature was noticed while doing data acquisition in the field and was quickly checked out by Jay Crawford. It is covered by alluvium with no nearby outcrop revealing its character. It is very shallow and should be exposed and geochemically sampled. This feature is separate from the feeder structure by 150 feet (~45m) and may strike to the northeast.

Deep Response

What appears to be lower resistivities and lower IP responses at depth are actually artifacts of the geometry between the electrode array and the dike-like features. When an electrode is either in, or very close to, a surface feature, all data acquired using that electrode are dominated by the characteristics of that feature. This is beneficial in interpretation as those characteristics are very diagnostic. However, if that surface feature is a vein, then all the data acquired from electrodes straddling and displaced from the vein have limited use because the surface has such strong influence. Some examples of this problem are shown in Appendix A. As a result, straddling electrodes on surficial features produce deep, low values. We consider this the "dead zone" and it is present beneath every well-defined, surficial, vein-type response. We see this characteristic on all lines which renders depth information moot.

Line 2 Data

Figure 6 displays the Line 2 Apparent Resistivity and Induced Polarization in logarithmic pseudosection. View is looking east. Warm colors are higher values; cool colors are lower values. Salient features are indicated by arrows.

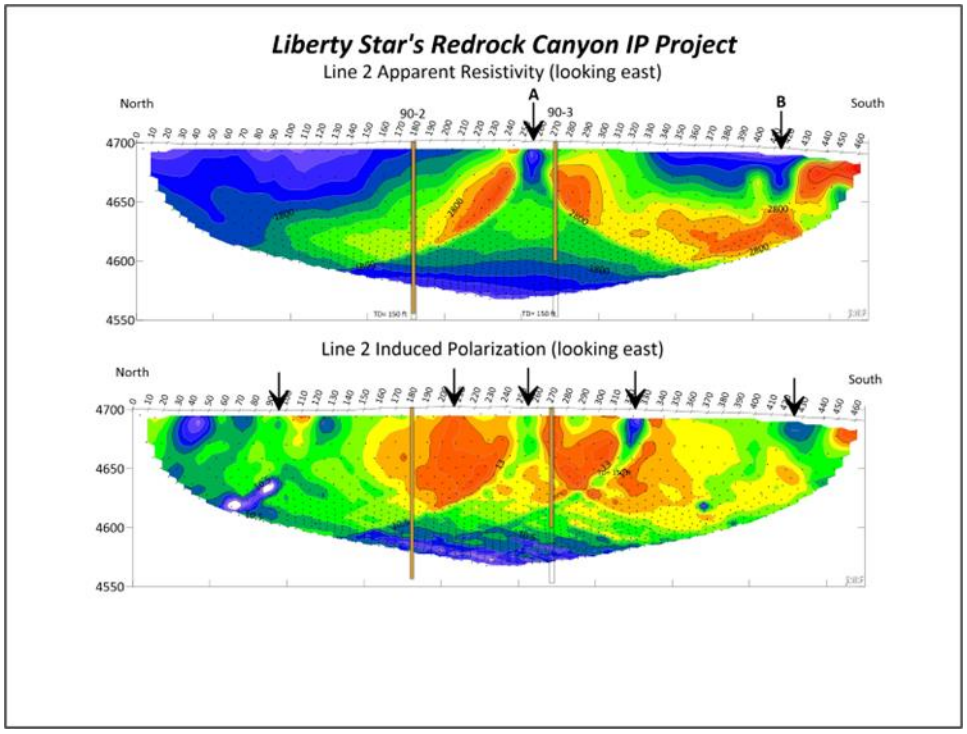

Figure 6: Line 2 Apparent Resistivity and IP raw data pseudosections
This pseudosection is hung on topography, looking east. See text for discussion.

Line 2 displays IP and resistivity response characteristics very similar to those of Line 1. There are now two main features in the resistivity data; the feeder structure A and the southern response B. The high IP response near the north end of Line 1, feature C, may project due East onto Line 2 but it is not as well defined. There is still a weak IP response at the projected location, hence the arrow in the IP section.

There are two older drillholes either on or close to Line 2; 90-2 and 90-3. Both of these holes are within or closely related to the high resistivity and high IP features. They were two of nine holes drilled in 1990 as part of a program performed by Primo Gold Ltd. to test surface geochemical anomalies. Drillholes 90-1 through 90-7 were angle holes oriented due east at an angle of 65° from horizontal. Holes 90-8 and 90-9 were vertical holes. Total depths ranged from 120 feet (37 m) to 150 feet (46 m). All holes were sampled for gold and silver at 5 foot (1.5 m) intervals. No other elements were sought.

Drillhole 90-2 is roughly located near Station 180 on Line 2. TD was 150 feet (46 m). In spite of its location well north of the feeder structure it had an average gold grade of 6.2 ppm for the first 40 feet (12 m). Gold values persisted to TD and overall averaged 2.1 ppm. In the entire hole there were only three intervals of non-detect (i.e. <0.005 ppm), all below 100 feet (30 m). The hole collared in limestone with significant jasperoid down to 40 feet (12 m), further supporting the relationship between gold mineralization and jasperoid. From 40 to 150 feet (12 to 46 m) the limestone maintained a reddish tint but the logger did not report jasperoid *per se*. Comparing the drillhole results with the IP data we see an excellent relationship, particularly for the first 40 feet (12 m) where the gold grades are the

highest. The jasperoid content of 25 to 33% down to 40 feet is not as well represented in the resistivity data but that is a lesser concern.

Drillhole 90-3 was located just south of the feeder structure by about 15 feet (4.5 m). Handheld GPS places it about five feet to the east of Line 2. Although it is much closer to the feeder than 90-2 the logger did not report jasperoid anywhere in the chips. However, red limestone was noted frequently down the hole. The near-surface gold assay values averaged 0.85 ppm for the first 40 feet (12 m) and sporadic values to the TD of 150 feet (46 m) averaging 0.43 ppm for the entire hole.

The central vein response A is the feeder feature seen on Line 1. On Line 2 it has migrated to the south centering about half-way between Stations 250 and 260. It still has the vein response characteristics as on Line 1 and is assumed to represent the same "feeder structure". The flanking response evident on both sides of the feeder structure suggest either a shallow spreading of the mineralization associated with the feeder structure or immediately adjacent additional veins that are also resistive and polarizable. This is especially noticeable in the IP data where a great deal of the line shows elevated IP. Some of the spreading character of the response can also be attributed to the angle between the line and the feeder structure but we lean towards additional veins because of the discreteness of the adjacent responses.

At the southern end of the line is feature B, another vein response, but with a bit more complicated appearance. Actually, the behavior of both the resistivity and IP data suggest that there may be another vein just off the end of the line that is resistive and polarizable.

Line 3 Data

Line 3 displays IP and resistivity response characteristics again very similar to those of Lines 1 and 2. There are now three main features in the resistivity data plus a suggestion of feature C at the north end of the line. Feeder structure A is still represented by its textbook response as we've seen on Lines 1 and 2. Feature B at the south end of the line continues to have a more complex signature but remains anomalous.

There is good evidence for another vein-type response just south of the feeder structure and is designated as Feature D. This could indicate a "horsetailing" or splaying of the feeder structure.

The high IP response near the north end of Line 1, feature C, may be related to this more subtle response on Line 3 but it does not correspond to a linear trend suggested by Lines 1 and 2.

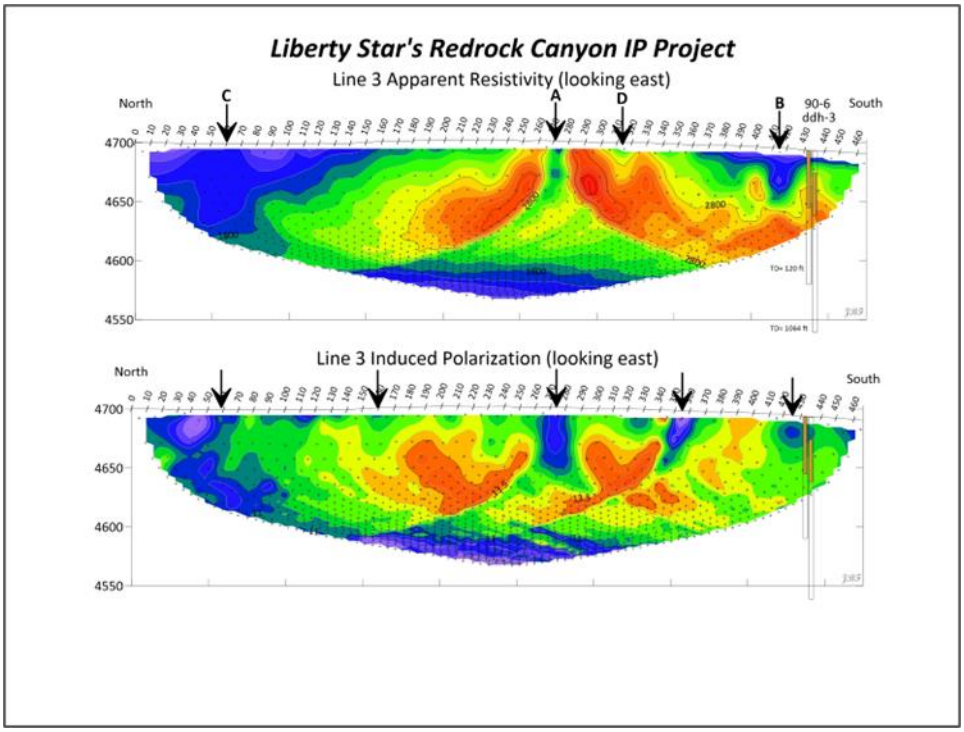

Figure 7: Line 3 Apparent Resistivity and IP raw data pseudosections, This pseudosection is hung on topography, looking east. See text for discussion.

Between Features A and C there are more high-resistivity and chargeability data suggesting additional veining, particularly so in the IP data. Another vein response shows up in the IP data between stations 350 and 360. These additional vein responses in the data help explain the broad isosurfaces seen in the 3D presentations of Figures 1 and 2.

Drillholes 90-6 and RCC-ddh-3 are located at the southern end of the line between stations 430 and 440. Drillhole 90-6 was drilled to 120 feet (37 m), at an angle, and ddh-3 to 1064 feet (324 m) vertically and both holes encountered gold within the first 50 feet (15 m). Average grade in the 90-6 drillhole was 0.231 ppm (0.0074 oz/ton) for the first 50 feet (15 m) and in ddh-3 average grade was 0.397 ppm (0.0128 oz/ton) for the first 55 feet (17 m). 90-6 was an angle hole at 65° below horizontal oriented due east (true depth of 109 feet or 33 m). ddh-3 was vertical and separated by perhaps no more than one foot (~30 cm) from the collar of 90-6. Interestingly, ddh-3 encountered no jasperoid or siliceous breccia in the first 150 feet (46 m). The upside for the geophysics is that there is good correlation between the resistivity and IP data and the assay results. A trench sample offset to the east and between Stations 430 and 440 was 17.3 ppm over 7.1 feet (2.2 m).

The central vein response A is the same feature seen on Lines 1 and 2, but on Line 3 it has migrated more to the south centering about half-way between Stations 270 and 280. It still has the vein response characteristics as on Lines 1 and 2 and is still assumed to represent the same “feeder structure” identified by Halterman. The approximate strike direction based on Lines 1 through 3 is N45W-S45E compared to Halterman’s N40W. Trench sample grades of 86.6 ppm over 5 ft (1.5 m) at Station 260 and 40.1 ppm over 6.7 ft (2 m) at Station 240, both associated with the feeder structure.

The flanking response evident on both sides of the feeder structure suggest either a shallow spreading of the mineralization associated with the feeder structure or immediately adjacent additional veins that are also resistive and polarizable. This is especially noticeable in the IP data where a great deal of the line shows elevated IP. Some of the spreading character of the response can also be attributed to the angle between the line and the feeder structure but we lean towards additional veining because of the "finiteness" of the adjacent responses.

Of the two rock-chip geochem samples within the grid, sample 314150 is located less than 10 feet (3 m) from Line 3 Stations 270 & 280 and well within the high resistivity zone associated with the feeder structure. Critical assay values are: Au 67.7 ppm (GRA), Ag 2.05 ppm (ME-MS), As 3200 ppm (ME-MS), Au >25 ppm (ME-MS), Fe 6.11% (ME-MS), and S 0.09% (ME-MS). These results suggest the polarizable material could well be arsenopyrite which in this environment is a gold indicator.

Feature B is the vein response at the southern end of the line. It does not have as well-defined a response as seen on Lines 1 and 2 but it is on trend. Additionally, the two drillholes, 90-6 and ddh-3, are located just south of the surface expression of the vein.

Geochemical sample 314146 (rock chip) is located near the southern end of the survey grid just east of Line 3 station 440. This places it right on a structure detected by the geophysics. Critical assay values are: Au 6.4 ppm (GRA), Ag 1.21 ppm (GRA), As 509 ppm (ME-MS), Au 6.1 ppm (ME-MS), Fe 1.81% (ME-MS), and S 0.02% (ME-MS). Again, an encouraging relationship between the geophysics and mineralization.

Additionally, half-way between Feature B and the feeder structure is a well-defined vein response in the IP data. Note the X shape beneath Stations 300 to 350. That shape results from the crossing of "pant-leg" responses due to multiple surficial features and offers further confirmation of multiple vein responses. This just shows how complicated the responses are becoming, especially in the raw data sections, as we progress through the lines.

North of the feeder structure are several less-well-defined, vein responses that clearly have elevated IP. This area is a good candidate for evaluating diffuse mineralization within the limestone. In addition, the strongest IP response in that area is directly in line with the favorable gold assays in drillhole 90-2 which is just 15 feet (4.6 m) or so west of Line 3

Line 4 Data

Line 4 displays IP and resistivity response characteristics in some places similar but mostly different from those of Lines 1 through 3. The well-defined feeder structure, if projected to Line 4, is missing. However, as suggested in Figure 4, we infer the feeder structure changes direction after passing Line 3 and trends southerly either alongside or possibly

passing under Line 4. A well defined vein response occurs between stations 390 and 400 and may represent the feeder structure A? turning southeasterly again.

There are now three main features in the resistivity data. Feature B at the south end of the line is questionable in the resistivity data but seems to be present in the IP data. The south end of all lines so far continues to be more complex than the area to the north.

There is good evidence for another vein-type response just south of the feed structure which was designated as Feature D on Line 3.

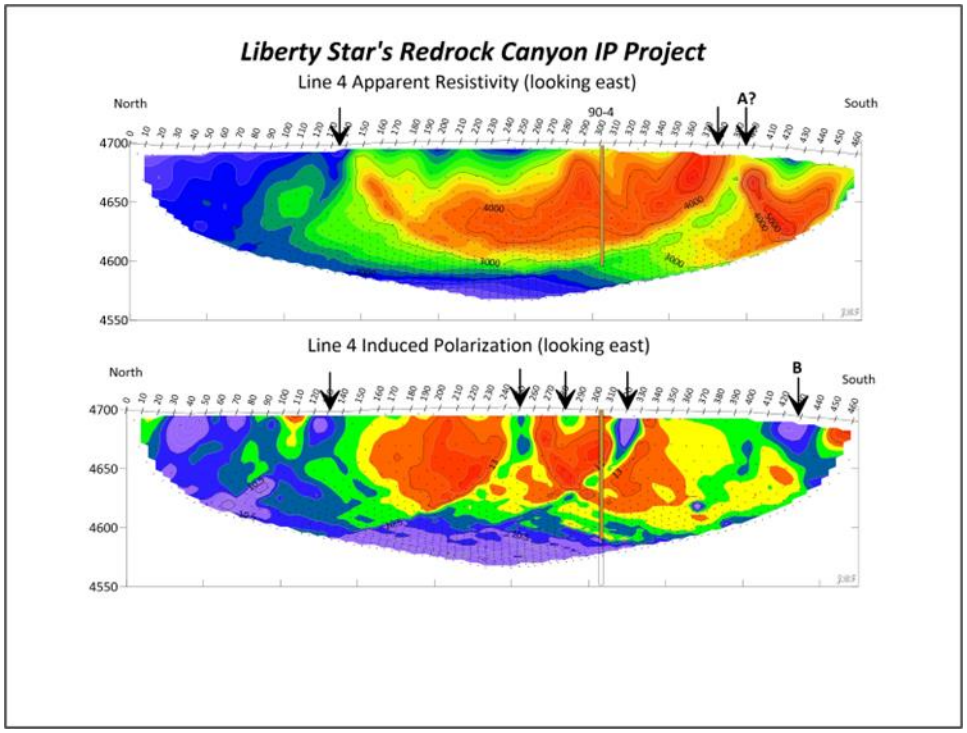

Figure 8: Line 4 Apparent Resistivity and IP raw data pseudosections
This pseudosection is hung on topography, looking east. See text for discussion.

As indicated in the plan view (Figure 4) the feeder structure is interpreted to follow an offset to the south. The inferred offset is the result of the lengthy high resistivity response in that area. In the Line 4 apparent resistivity sectional data we lose the well-defined character and features A and C seen on Lines 1 through 3. There is a vein response near Station 250 in the IP data that could represent the feeder structure but it occurs to the north of where the projected trend would intercept Line 4. Consequently, we interpret the large high-resistivity feature to correspond with that *offset portion* of the feeder structure. In other words, the feeder structure is either closely paralleling Line 4 or passing under it at a very shallow angle.

Additionally, the aforementioned features at the southern ends of the lines appear to continue but remain complex. A vein signature is assigned feature B in the IP section.

The only drillhole directly associated with Line 4 is 90-4 and is located near Stations 300 and 310 around 5 feet (1.5 m) to the east of the line. Gold assays for the first 105 feet (32 m) in 90-4 averaged 0.301 ppm (0.010 oz/ton). Extensive high resistivity and IP data in the vicinity of 90-4 strongly support the relationship between those electrical properties and the presence of jasperoid, sulfides, and gold. The lithology log for 90-4 confirms jasperoid or hematite-stained limestone for the length of the hole. In turn, this may indicate that the hole is within or very close to the feeder structure, as we propose.

High resistivities and elevated IP responses occur over much of Line 4. Many of those responses suggest the presence of either at surface or very near surface target material. This is a good situation for building volume gold but has the minor disadvantage of making three-dimensional, and two-dimensional, inversions much more difficult than buried targets. As the multiple arrows, particularly in the IP section, indicate there are several locations that might benefit from additional surface geochemistry.

Line 5 Data

Line 5 presents a rather different appearance compared to the first three lines in both resistivity and IP response. There is a single, well-defined vein response, A?, at the southern end of the line that we propose is the evidence of continuance of the feeder structure. The remainder of the line from that point to the north appears to be dominated by many minor vein-type responses resulting in a smeared-out appearance of high response, again, in both resistivity and IP data.

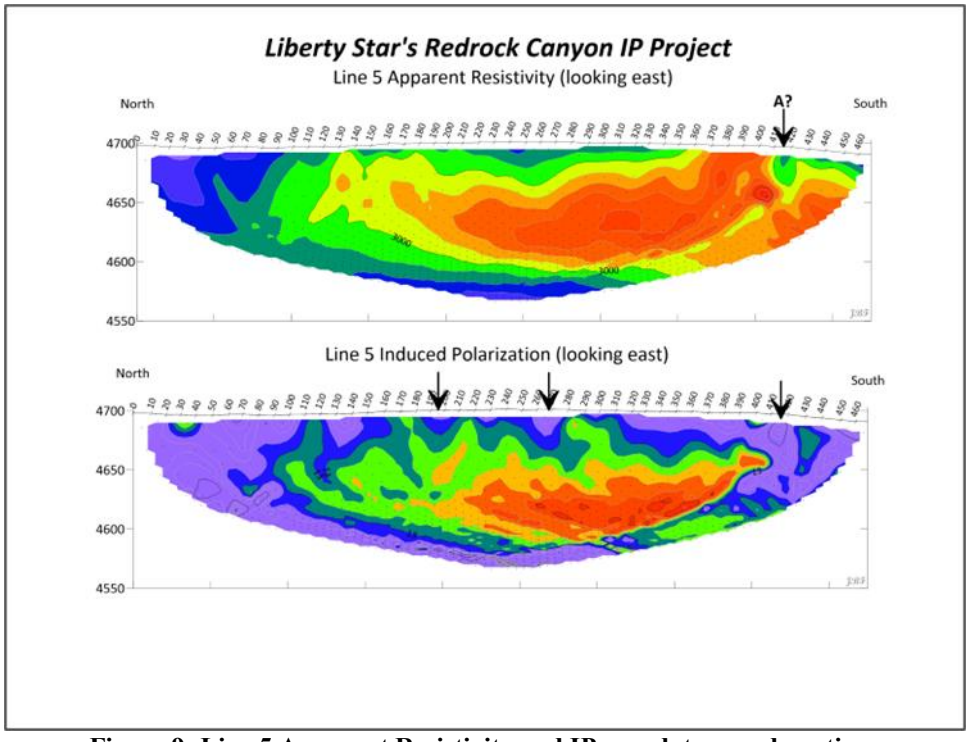

Figure 9: Line 5 Apparent Resistivity and IP raw data pseudosections
This pseudosection is hung on topography, looking east. See text for discussion.

The single drillhole most closely associated with Line 5 is 90-1 which was collared about 10 feet (3 m) east of Station 110. Like all other drillholes within the grid it has anomalous gold assays averaging 0.077 ppm (0.0025 oz/ton) for the first 40 feet (12 m). However, it is angled away from the survey line, so it is not indicated on the image. It is included, however, in the 3D images, Figures 1 and 2.

3D Data

Three-dimensional Inversions

One of the goals of the IP test survey was to create a three-dimensional (3D) view of the subsurface based on the resistivity and IP data acquired over existing drillholes such that the data could be compared with the lithology logs and assay data from those drillholes. However, as we have indicated, the test grid turned out to be underlain by multiple, steeply-dipping, mineralized veins either cropping out or nearly so. As encouraging as it is to have that much mineralized material present, it also presented a problem when the inversion processing began.

A first comment is that most inversion software used for resistivity and IP forward and inverse modeling (especially the latter) is oriented around the optimal visualization of buried bodies. The majority of inversion software packages use finite element solutions. The algorithms employed are typically intended to provide a certain degree of smoothness to the results. Thin outcropping mineralized veins violate this approach because the associated gradients are much higher at surface than the software allows. This problem manifests itself in the blurring or blending of surface features such that the individual veins are not well represented. There are countless ways to adjust the inversion parameters but achieving accurate reconstruction of the veins in the final models was a challenge.

Two different inversion software packages were used. Sub Rosa's inhouse software package is ERT*lab*64 by Geostudi Astier. An alternate test was run by hydroGeophysics, Inc. software package ResMod3DInv by Geotomo Software. Our preferred results are presented below.

The effect mentioned regarding the blurring and blending of surficial responses is apparent in all three images. However, these results, although lacking in definitive vein presentation, offer an alternative view of how the vein-associated mineralization is diffused into the hosting limestone which may represent a more volumetric situation that is more desirable for mining.

Overview of the inversion process

This section provides a very high level overview of the resistivty inversion process using the ERT*lab*64 software. The software processes the raw data to create a model of the subsurface resistivity distribution. The data flow is performed in the following sequence.

1. Input Data: ERT*lab*64 takes apparent resistivity measurements collected from the field, and then it generates an initial model based on these measurements, in addition to the initial starting parameters input by the user in the starting model or initial model. This initial model is then refined through iterative calculations.
2. Synthetic Data Generation: The software simulates what the resistivity data would look like if the initial model were accurate.
3. Model Adjustment: ERT*lab*64 then compares the synthetic data to the actual measurements and adjusts the model accordingly.
4. Iteration: Steps 2 and 3 are repeated until the model closely matches the observed data.
5. User review: The user must then review the results, and if not reasonable, new starting parameters for the initial model will be selected, and then the above steps will be repeated.

ResMod3DInv Resistivity Image

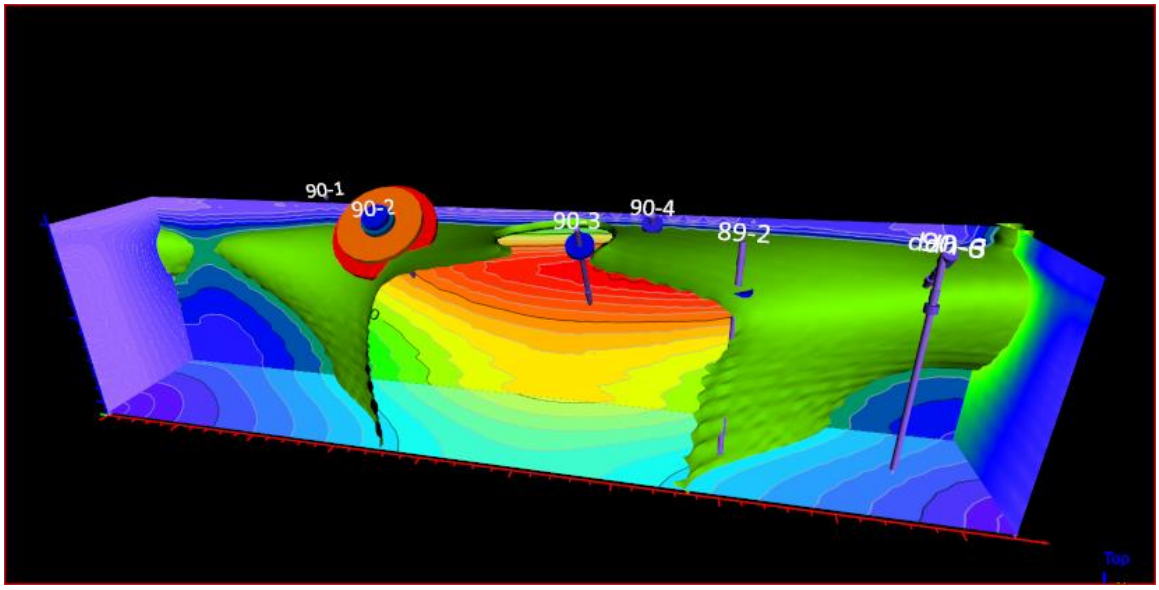

Figure 10: Redrock Canyon ResMod3DInv 3D resistivity image.

A three dimensional view of inverted resistivity data with relevant drillholes is presented in the Figure above. The green isosurface encloses resistivities greater than 10,500 ohm-meters and encompasses the area of most intense veining. The view is looking easterly. Drillhole gold assays are scaled by value; red is the highest of these holes at 15 ppm.

This image illustrates a "blending" effect the inversion routines create as compared to the raw data. The concentrated area highlighted by the isosurface is understandable in the context of multiple vertical features concentrated in the central and southern portions of the survey area.

ERTlab64 Resistivity Image

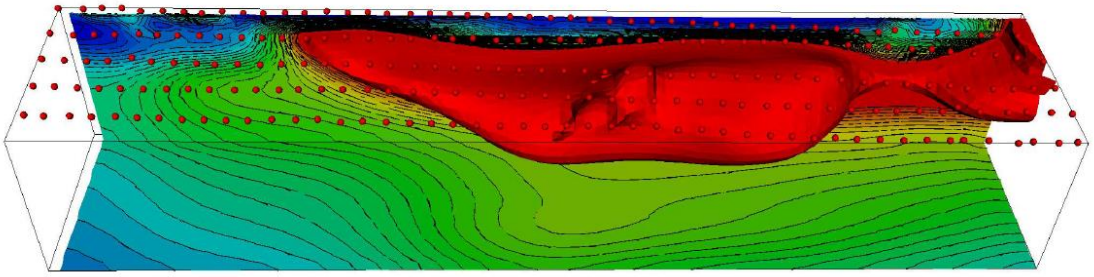

Figure 11: Redrock Canyon 3D ERT*lab*64 resistivity image.

As can be seen there are a number of similarities between the ResMOD3DInv and ERT*lab*64 inversion results. We note the bulk of the responses are near the surface and are concentrated around the middle and towards the south of Lines 3, 4 and 5. We would also note in this image there is not as much information at depth which is to be expected given the reasons described earlier in this report. We caution the reader that there is likely to be less homogenenaity in actual subsurface results than that indicated by imaging, which creates the impression of a connected, uniform volumetric area. The inversion software is taking finite, discrete vertical features and combining them into one volume with a bias towards horizontal layering.

ResMod3DInv IP Image

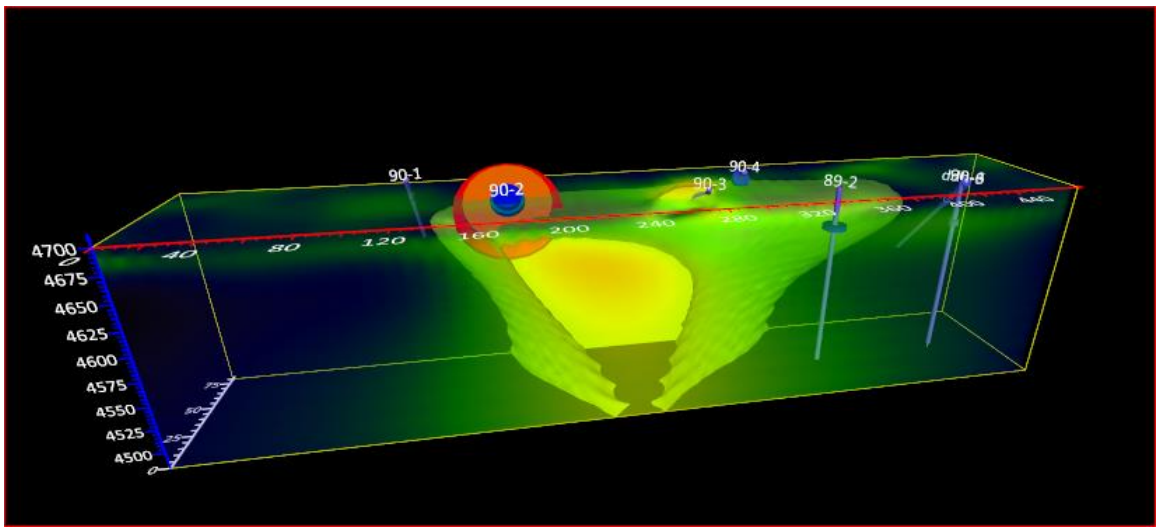

Figure 12: Redrock Canyon ResMod3DInv 3D IP image.

The Figure above displays a similar isosurface of the IP data enclosing the volume of higher chargeabilities. The extension to depth in both examples is questionable and may result from the masking effect of the extensive veining at surface.

Recommendations

In light of the successful completion of the IP test survey we suggest the following possible courses of action.

1. Depending on the desire to continue mapping gold-mineralized vein structures subsequent IP surveying may be considered. It is recommended that a portable IP system employing the same array configuration be used. Various options exist. Due to the thinness of the veins encountered during the test it is hard to recommend expanding the array spacing from 10 feet to anything larger. However, this is offset by using a lightweight, portable system that can perform traverses rapidly and expeditiously. Such systems are common in the industry. Extending the test grid westerly tracking the feeder structure towards the rhyolite outcrop may reveal additional veins that are presently beneath alluvial cover. In addition, extending the test grid to the east following the projected trend of the feeder structure in that direction may also reveal more mineralized veins presently not visible due to soil cover. Additional options might be to extend the test grid to the north and south for the same reasons already stated.

2. An option already discussed and partially in motion as this is written is to test a shallow-sensing electromagnetic (EM) system. We have already established that the mineralized veins have physical property contrasts with the hosting limestone.

It is feasible that these same physical properties, or some not tested yet, may be detectable by such a system. These systems are highly portable, operated by a single individual, and provide very rapid coverage, much faster than IP and resistivity which require installing electrodes. The biggest shortcoming is needing to mark the lines to be covered. Dr. Gail Heath has provided a GSSI Profiler and it is presently in Tucson. It will need a data-logger that is being pursued.

3. After reviewing some previous geophysics performed at the Redrock Canyon site by MinSearch, we reprocessed some of their very-low-frequency (VLF) electromagnetic coverage. As with the aforementioned Profiler, a VLF instrument is highly portable, operated by a single individual, and can perform rapid traverses. MinSearch's VLF data were acquired with a 300 foot station separation which is far too large to be able to sense the thin veins confirmed by the IP. We suggest renting a VLF system and performing tests over the IP grid to see if VLF might also be useful. Both the Profiler and VLF are EM systems but operate on a quite different basis; the Profiler is a combination transmitting loop and receiving loop in a single instrument 4 feet (1.3 m) long. The VLF system uses distant submarine transmitters (typically Seattle, WA and Cutler, ME) as their source so the surveying instrument is just a receiver. VLF has very much greater depth of investigation than the Profiler but has some limitations that can impact when surveys can be run. The strong points for both systems are that they are inexpensive, rapid and provide data relatively easy to understand.

4. A non-geophysical recommendation would be to more accurately survey the existing drillholes. We, and Liberty Star, have multiple handheld GPS locations for the drillholes (over most of the Hay Mountain project area) which are probably adequate. The shortcoming is elevation. Handheld GPS systems are not that good at elevations. Having accurate elevation control is necessary for creating digital presentations, especially if 3D, using the drillhole assay data and lithologic logs. Repeat surveying using *survey-grade* GPS systems is recommended. There are still some minor loose ends about the precise collar locations and names which might be resolved by spending more time at each drillhole location searching for the actual collar.

5. For the same reasons stated above regarding survey accuracy and, more importantly, improved geologic mapping should be performed. The current base maps are strongly dependent on Gilluly's 1956 U.S.G.S. Professional Paper which was based on much earlier work begun in 1936 and completed in 1940. Subsequently those early results were transferred to 1950s 15 minute topographic sheets for inclusion in the 1956 paper, which is what we're currently using, if we're using Gilluly's geology. Updated mapping should be a consideration.

6. Another option well worth consideration is LIDAR mapping. LIDAR provides very high precision elevations and spatial coverage. Since the gold mineralization is associated with veining and structural features, LIDAR can highlight these features. LIDAR can be flown via drones, helicopters and-or fixed wing aircraft. It would be

one of the more expensive options to consider but most of the Hay Mountain, Zebra and/or Redrock Canyon areas can be covered in a single flight producing long lasting data.

Useful References

Elliot, Charles L., 1967, **Theoretical Curves of Induced Polarization Response and Apparent Resistivity,** private publication by Canadian Aero Mineral Surveys Ltd., Tucson, AZ & Ottawa, Canada.

Fink, James B., 2022, **Review of Historic Induced Polarization and Resistivity Data for the Redrock Canyon Project, Cochise County, Arizona**, unpublished internal report.

Gilluly, James, 1956, **General Geology of Central Cochise County, Arizona**, U.S.G.S. Professional Paper 281, U.S. Gov. Printing Office, Washington, D.C.

Halterman, Leroy, 1988, **Report on The Zebra Property, A Gold Prospect, Cochise County, Arizona**, internal report prepared for Tempo Resources Limited by MinSearch, Inc., Albuquerque, NM.

Halterman, Leroy, 1991, **Report on The Zebra Property, A Gold Prospect, Cochise County, Arizona**, internal report prepared for Primo Gold Ltd. by MinSearch, Inc., Albuquerque, NM.

Lovering, T. G., 1972, **Jasperoid in the United States – Its Characteristics, Origin, and Economic Significance**, U.S.G.S. Professional Paper 710, U.S. Gov. Printing Office, Washington, D.C.

Rasmussen, Jan C. & Hoag, Corolla K., 2011, **Hay Mountain Exploration Report, Tombstone District, Arizona**, unpublished internal report by SRK Consulting Inc. for Liberty Star Uranium & Metals Corp.

APPENDIX A

In this appendix we review numerous aspects of data processing, from statistics through inversion modeling.

Data statistics

Figure A1 is a histogram of the observed apparent resistivities for all 5 lines. A first approximation of the histogram would be that of a Gaussian distribution but there is a noticeable skewness on the upper side of the histogram. We attribute these higher-than-average resistivities to the presence of jasperoid and siliceous breccia. Although the resistivity contrast between the limestone and jasperoid veins is not that great, it is sufficient to allow statistical separation.

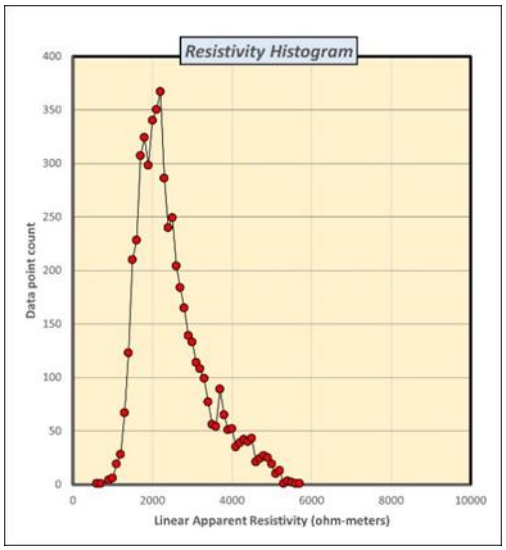

Redrock Figure A1: Linear histogram of apparent resistivities in ohm-meters.

An alternative way of looking at the resistivity histogram is to use the logarithmic values of the resistivities as shown in Figure A2. The red line signifies the bulk or average distribution of the data while the blue line isolates the "anomalous" data; i.e. the higher-than-average values. The thin black line is the difference between the fitted PDFs and the original data showing the quality of fit. This approach to analysis influences how the subsequent data plots are viewed.

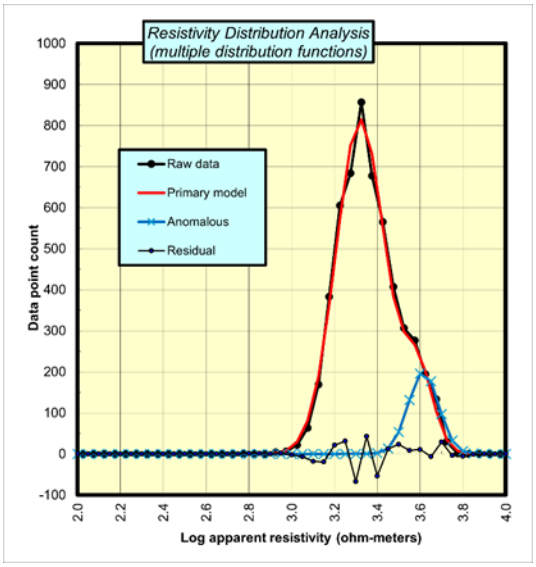

Figure A2: Histogram of logarithms of apparent resistivities including PDFs fitted to the data.

A histogram of the IP values is shown in Figure A3. The average IP response was 11.9 ±1.8 millivolts/volt. A simple Gaussian distribution function fits the bulk of the data very nicely. However, as with the resistivity data, the overall distribution is skewed to the upside. This simple observation indicates a relationship between higher-than-average resistivities with higher-than-average IP values. In other words, it conclusively demonstrates that the jasperoid and siliceous breccia contain the mineralization, most likely metallic-luster sulfides. The "anomalous" IP values can be further identified by a separate PDF as shown in Figure A3. The average value for the anomalous IP PDF is 15.0 mV/V which is 25% higher than background. This bodes well for using IP as a mapping tool in this environment.

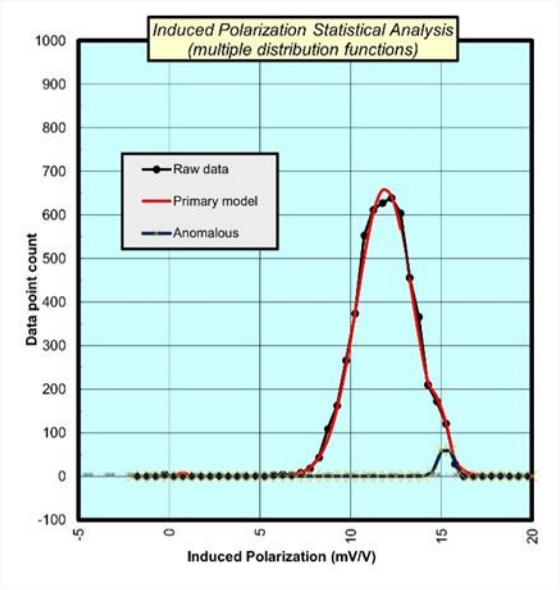

Figure A3: Histogram of IP values with fitted PDFs

However interesting the statistical aspects of the data are, they don't provide any spatial information. For that, we need to look at the raw data plan views and profiles.

Vein Signature Discussion

Prior to discussing the data in more detail, a particular issue needs to be pointed out. Several of the interpreted veins follow what appear to be local lows in the apparent resistivity map and in many of the sections. Many of the veins also show up as very localized IP lows. Both of those effects are due to the interaction of the electrode array and the thickness of the veins. If an electrode is placed in a thin, resistive, polarizable vein then it will result in a high data value in both the resistivity and IP. If the same vein is located *between* two electrodes, then it produces *low* values. It's a matter of geometry. This has long been an issue for data inversions because the "thickness" of the vein is frequently not reflected in the default cell-size used in finite element inversion software. In order to accurately reproduce the true response character of a vein (in inversions), the thickness of the vein *must be greater* than the electrode separation. The simplest solution is to view the raw data for such effects prior to inversion and adjust the cell sizes accordingly. Alternatively, detailed forward modeling can be employed but in both cases it pushes the limits of normal data processing.

To further illustrate the issue some theoretical curves done back in the 60s for the pole-pole array over vertical dikes (Elliot, 1967) offer some insight. The curves represent the theoretical response, in this case, for apparent resistivity over dikes of varying thickness relative to the electrode spacing. Curves are presented for ratios of thickness (w) versus electrode spacing (a) for 0.1, 0.2, 0.5, 1.0, 2.0 & 5.0. Note that all curves for w/a less than 2 have a low central value when the electrodes straddle the dike. So, for the survey at hand,

dikes or veins of thickness less than 10 feet, there should be a low response when the electrodes straddle it; which is precisely what we see in most of the raw data sections.

The singular most important result of the IP test is the discovery of vein targets beneath soil cover where they have not been previously detected, and, that this was done in such a small area, much of which was exposed bedrock. This proves advantageous in guiding geochemical sampling as well because so many veins have not been tested due the thin veneer of soil hiding them.

These features are right at surface and are just beneath inches of soil and should be easy to test. However, the presence of so many surficial features has created an unanticipated inability for us to obtain information at depth. The surface features mask the deeper responses the same way the front row of trees masks the depth of the forest

As explained in the report, the pseudo-sections of raw data unequivocally display the almost text-book responses of thin, vertical, dike-like features in both the apparent resistivity and IP data. This is not surprising as previous mapping and geochemical surveys had already established that gold mineralization was associated with jasperoidal and siliceous veins. We specifically located the IP test site over existing drillholes with known gold mineralization in order to be able to correlate the IP and resistivity results with the geologic logs and assay data.

Upon reviewing the unprocessed raw data for Line 1 while still in the field it became obvious that there was a significant anomaly in the middle of the line. Subsequent processing and plotting of the data that first evening confirmed we were seeing a thin, vein-like feature that was more resistive than the surrounding limestone and had an associated IP response, which is precisely what we were hoping to see, and continued to see in the remaining four lines.

The manner in which resistive, polarizable veins (dikes) manifest themselves in data sections and-or profiles is the primary reason for this appendix. Their response is contrary to what common sense might dictate. Simply stated, a resistive dike, if thin enough, relative to the electrode spacing, will produce an abnormally low resistivity response when in-between electrodes. Likewise for polarizability. These contrary results have caused considerable discussion and disagreement over the years and pose a challenge to computer inversions.

The low response occurs when the two electrodes are straddling the vein. Prior to the advent of computers in the field we were constrained to using previously calculated theoretical curves of ideal situations. In retrospect, those curves were great teaching aides. Figure A5 is an example of the theoretical response of a pole-pole array over thin, resistive, vertical dikes crossed orthogonally.

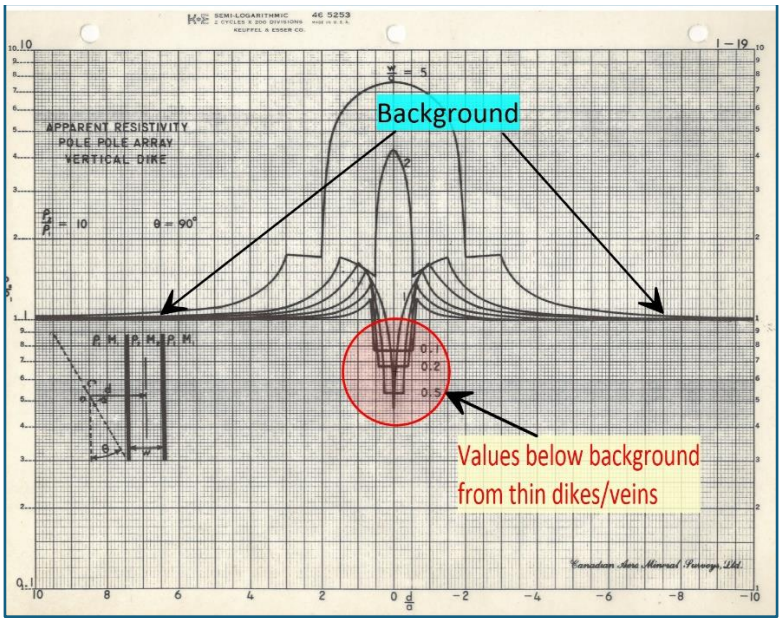

Figure A5: Theoretical response curves for a pole-pole array crossing a thin, vertical dike with a resistivity contrast of 10 to 1.

The key take-away here is that even if the dike is as wide as the a-spacing (10 feet in our case) there is still an abnormal low involved.

In pseudo-section form the appearance of a thin resistive dike becomes easy to recognize. Line 1 is an excellent example. Figure A6 shows three vein responses that are subtly different.

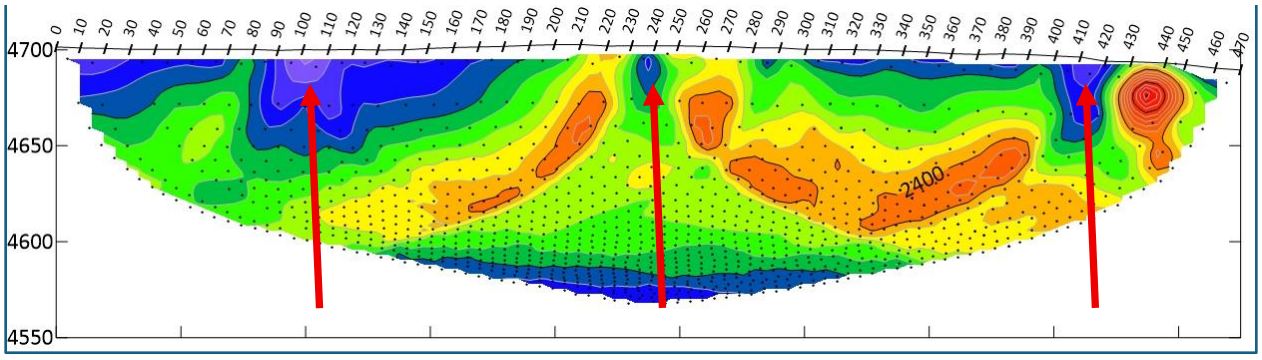

Figure A6: Logarithmic pseudo-section of Line 1 apparent resistivity data. Warm colors are higher values; cool colors are lower values. Background resistivity is roughly 1,850 ohm-meters. Interpreted vein responses indicated by red arrows.

The three veins identified in Figure A6 can be seen in the pseudo-section but, due to variable geology around them, they present subtly different appearances from each other. The central "lows" in each case almost precisely locate the veins. Additionally, what is also evident are the higher-valued "pant legs" as indicated in Figure A6 going down and away

from the surface expression of the veins. The data between the pant-legs contains very little information at depth due to the masking effect of the veins. This area between the pant-legs is considered the "dead zone" for that reason. Obviously, if there are enough veins with similar physical properties, they can prevent the detection and characterization of deeper features. The cooler colors at the bottom of the section are the result of over-lapping dead-zones and exemplify that this is an area with no useful data.

An alternative view of the veins is with single-electrode-spacing profiles. Figures A7 through A16 show the apparent resistivity and chargeability for all five lines for the electrode spacings of 10 to 60. The vertical scale is consistent for all the resistivity figures. Only Line 1 chargeability (Figure A8) has a different vertical scale.

Figure A7 shows 6 stacked profiles from Line 1 apparent resistivity.

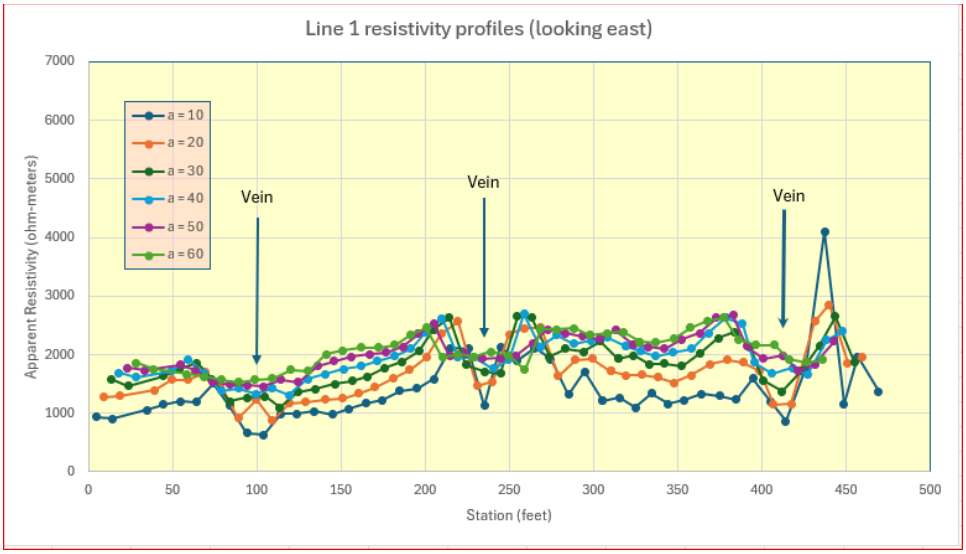

Figure A7: Line 1 apparent resistivity data in profile form, looking east. The three veins noted in the pseudo-section are indicated. The legend explains the electrode spacing.

Figure A8 shows the same 6 stacked profiles from Line 1 for chargeability. Note the absence of IP response associated with the rightmost (southern) vein identified in the resistivity profile. The northernmost vein IP response is the highest in the entire survey.

Line 1 was the first line run during the survey. We processed the data in the evening and saw the strong response. First thing next morning Jay Crawford and Jim Fink checked out the location and found it completely covered with alluvium for tens of feet around it. Obviously, it is one of the many hidden veins in the area. We regard this as an unmitigated success for IP. We look forward to learning what's under the thin veneer of alluvium.

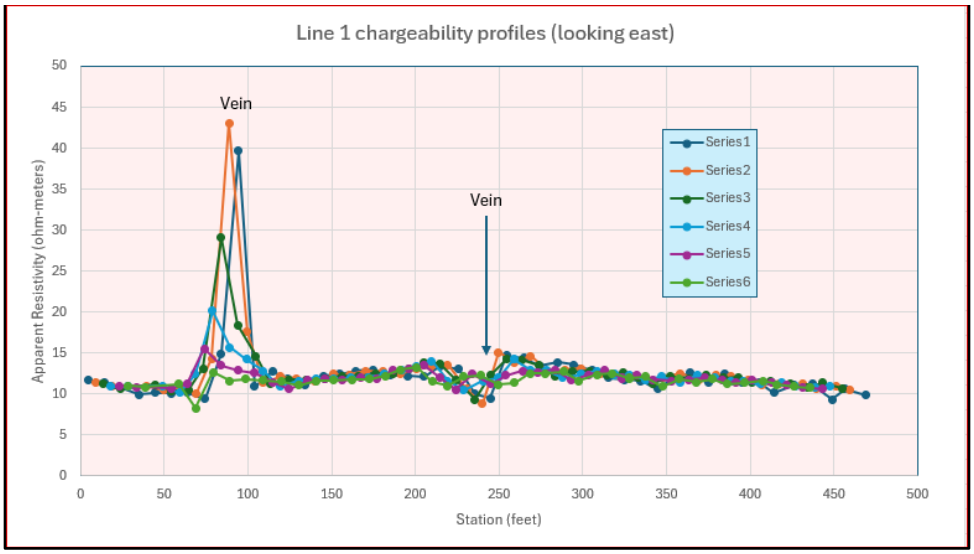

Figure A8: Line 1 chargeability data in profile form, looking east. Only two veins noted in the pseudo-section are indicated. The legend explains the electrode spacing. The leftmost (northern) vein response is the highest response in the survey.

Line 2 apparent resistivity is presented in Figure A9 below. Note again the differences in the appearance of the vein signatures. The proposed vein on the southern end of the line presents a very complicated signature. There also seems to be an additional vein just south (to the right) of the central vein. Both it and the north vein have subdued signatures, but are still evident.

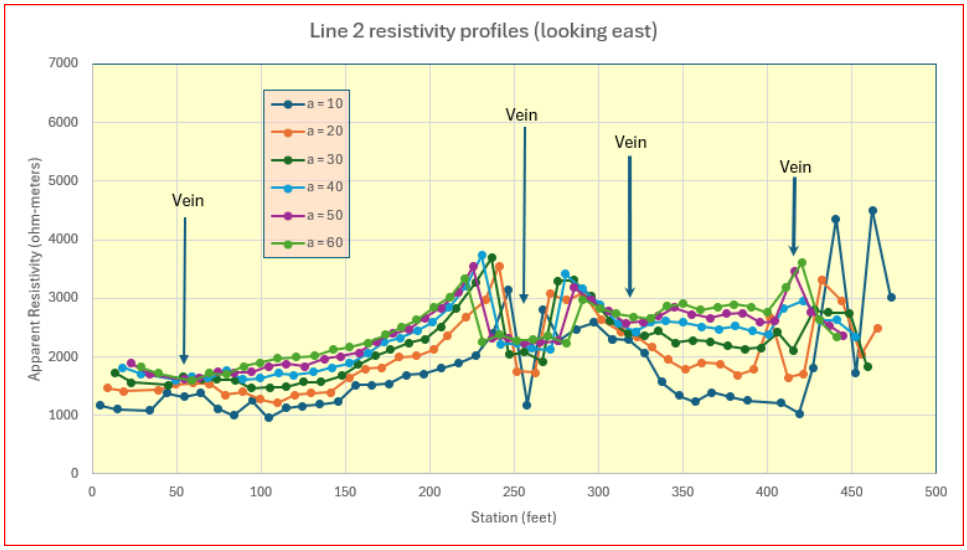

Figure A9: Line 2 apparent resistivity data in profile form, looking east. Four veins are suggested. The legend explains the electrode spacing.

Figure A10 shows the stacked profiles from Line 2 for chargeability. Note the minimal response in the IP profile associated with the rightmost (southern) vein (not marked here) identified in the resistivity profile. The central vein is still well defined but the two other veins are less well defined.

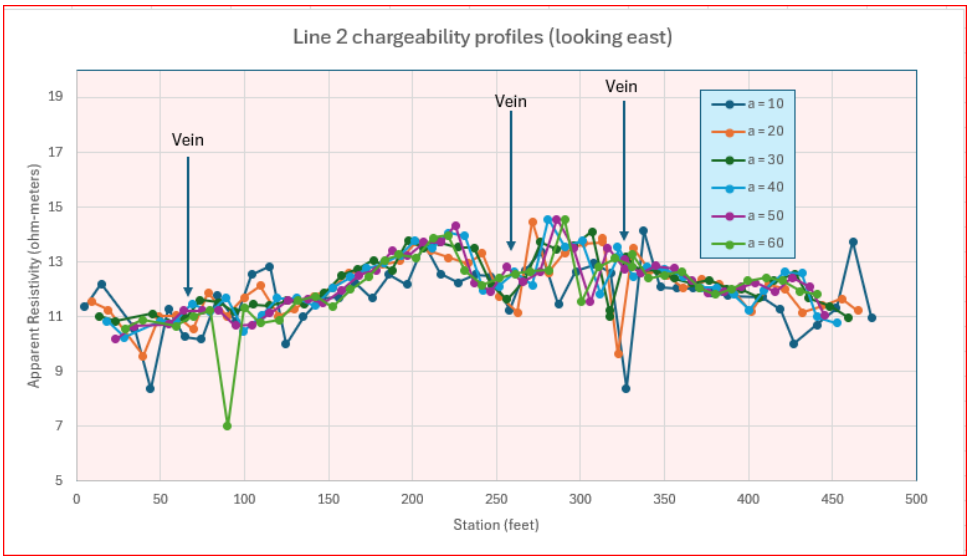

Figure A10: Line 2 chargeability data in profile form, looking east. The vein signatures are not as well defined as in the resistivity data. The southern vein is not included because it is too difficult to localize.

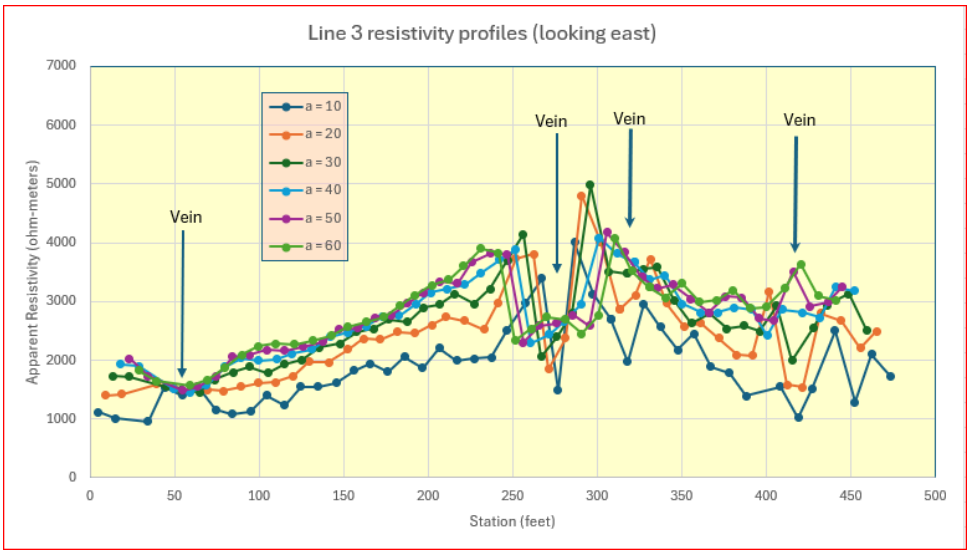

Figure A11: Line 3 apparent resistivity data in profile form, looking east. Four veins are suggested. The legend explains the electrode spacing.

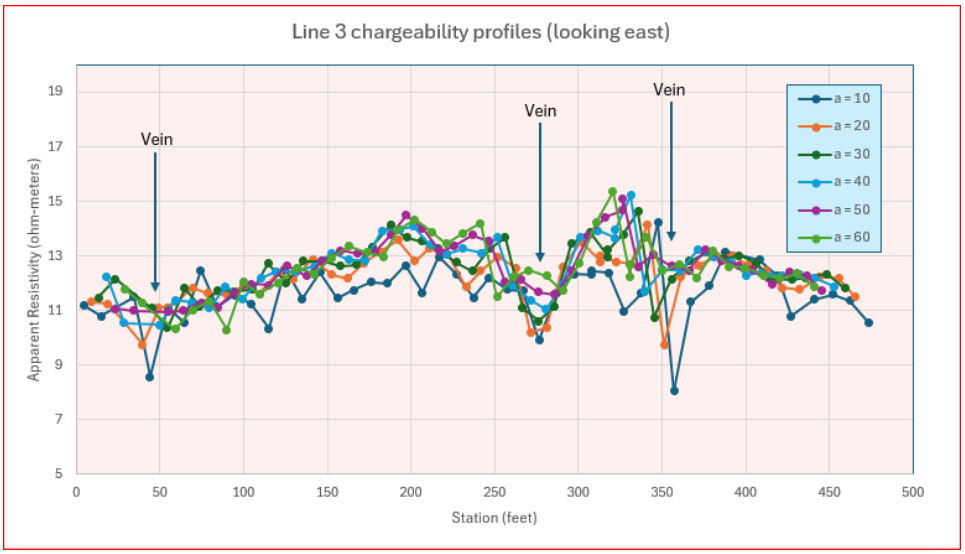

Figure A12: Line 3 chargeability data in profile form, looking east. The vein signatures are not as well defined as in the resistivity data. The southern vein is not included because it is too difficult to localize.

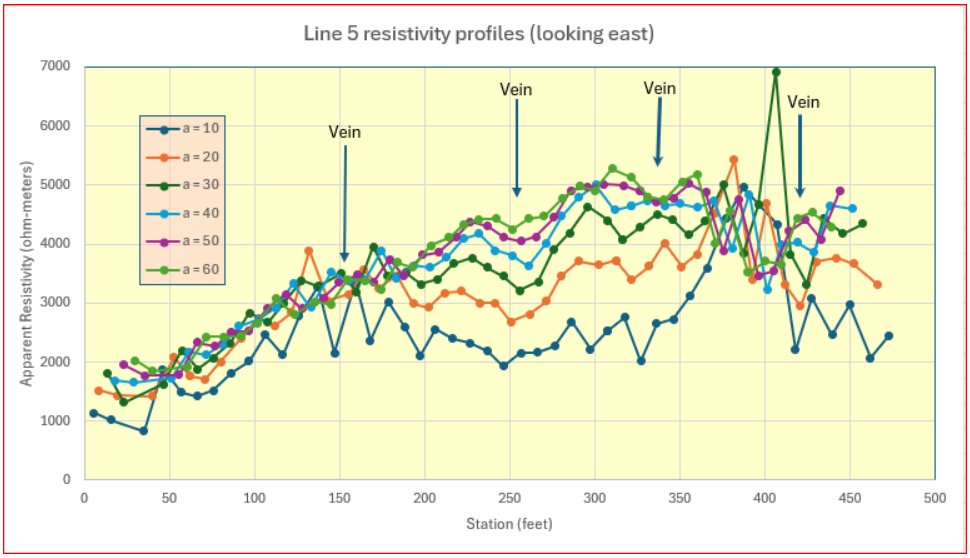

Figure A13: Line 4 apparent resistivity data in profile form, looking east. Four veins are suggested. The legend explains the electrode spacing.

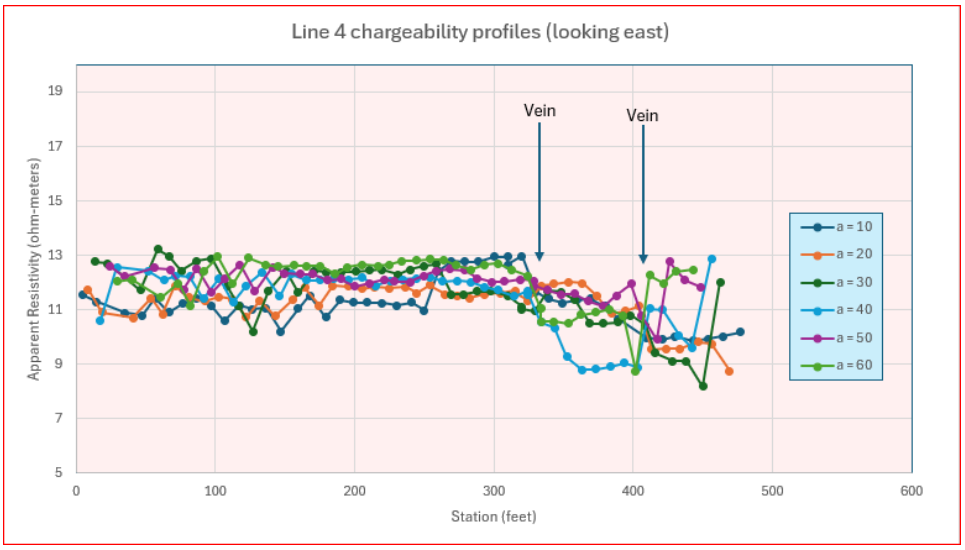

Figure A14: Line 4 chargeability data in profile form, looking east. The vein signatures are not as well defined as in the resistivity data. The southern vein is too complicated to be specific about location. The feeder structure (central vein) is poorly defined but is suspected to be the vein around station 340. The north vein is also non-descript.

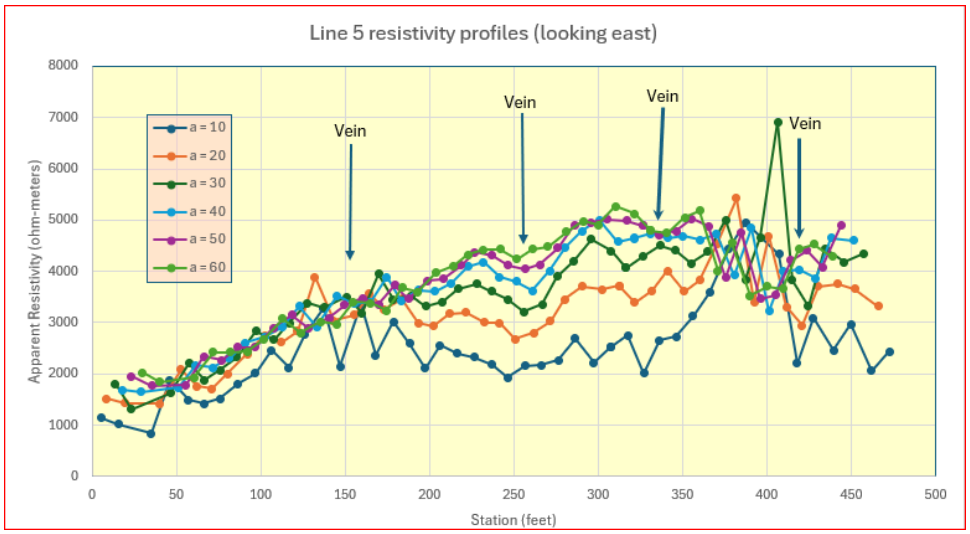

Figure A15: Line 5 apparent resistivity data in profile form, looking east. Four veins are suggested. The legend explains the electrode spacing.

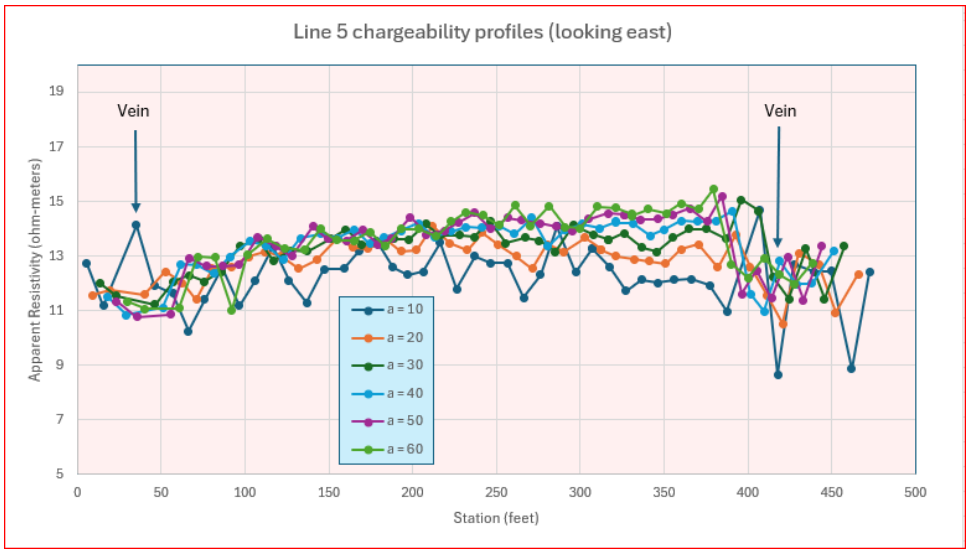

Figure A16: Line 5 chargeability data in profile form, looking east. With the exception of the southernmost vein, or structure, no other veins are evident.

Inversion Modeling

It would be helpful to discuss the inversion results versus raw data; both of which are presented in the body of the report. Ordinarily, raw data are usually relegated to an appendix and the focus of discussion in the main body of the report is on the inversion results. In this particular situation the raw data are far better at illustrating the vein character of the site. The inversion process tends to blur and blend which produces a more volumetric result at the expense of localized veins. In short, inversion algorithms are not good at producing near-vertical features, especially when such features are visible on the ground surface. This is not an impossible task, just exceedingly time-consuming and requiring in-depth knowledge of the inner workings of inversion software as well as the facility to adjust those workings which aren't generally accessible.

In comparison to the pseudo-sections and profiles the following inversion results are presented. Each line is presented on the same format as the raw data with the drillhole symbols and vein markers unchanged in position. This allows a one-to-one comparison and provides some insight into the difficulties the inversion software has with vein-type signatures. Occasionally there are good correlations but frequently not. This led to considerable effort in trying optimize the inversion runs to produce vein-like results but with limited success. In a few examples there are some colored-in areas that indicate extreme values. They are colored in to avoid extreme crowding of contour lines.

Line 1 Inverted Sections

Line 1 resistivity shows a good correlation with the feeder structure in the center of the line. The vein at the south end of the line is not represented. Vein C at the north end has a hint of recognition but it is only weakly indicated in the raw data anyway.

One of the concerns with the aforementioned vein signature is reflected in the IP section at the location of the feeder structure. The narrow low values produced by thin, resistive, polarizable veins appear in the inverted section as a low. The software should have eliminated it and produced a narrow high response. Further, the flanking high zones are shown as separate highs whereas they actually should be represented as a single high. The B and C veins are barely, if at all, represented.

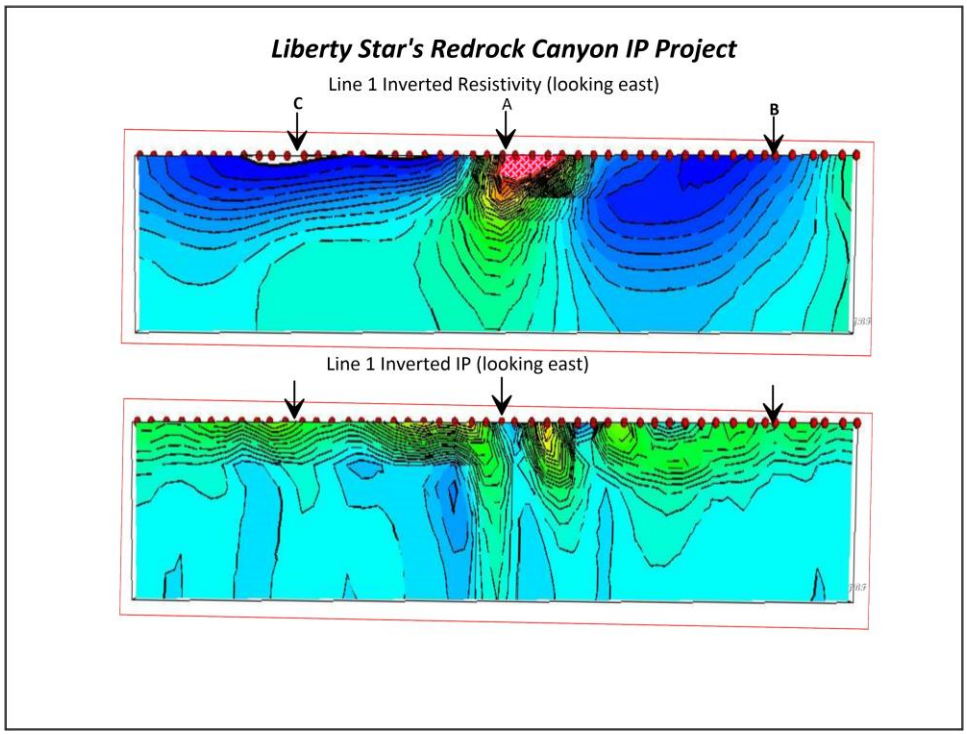

Figure A17: Line 1 inverted sections, looking east.

Line 2 Inverted Sections

Line 2 resistivity shows a correlation with the feeder structure (feature A) in the center of the line but is considerably broader than that of Line 1. Nevertheless, it presents a downward trend as expected for a near vertical vein. The vein at the south end of the line (feature B) is, at best, represented by a gradient in the resistivity. Vein C at the north end has no expressions but the northern area is, in general, of lower resistivity and corresponds with the raw data.

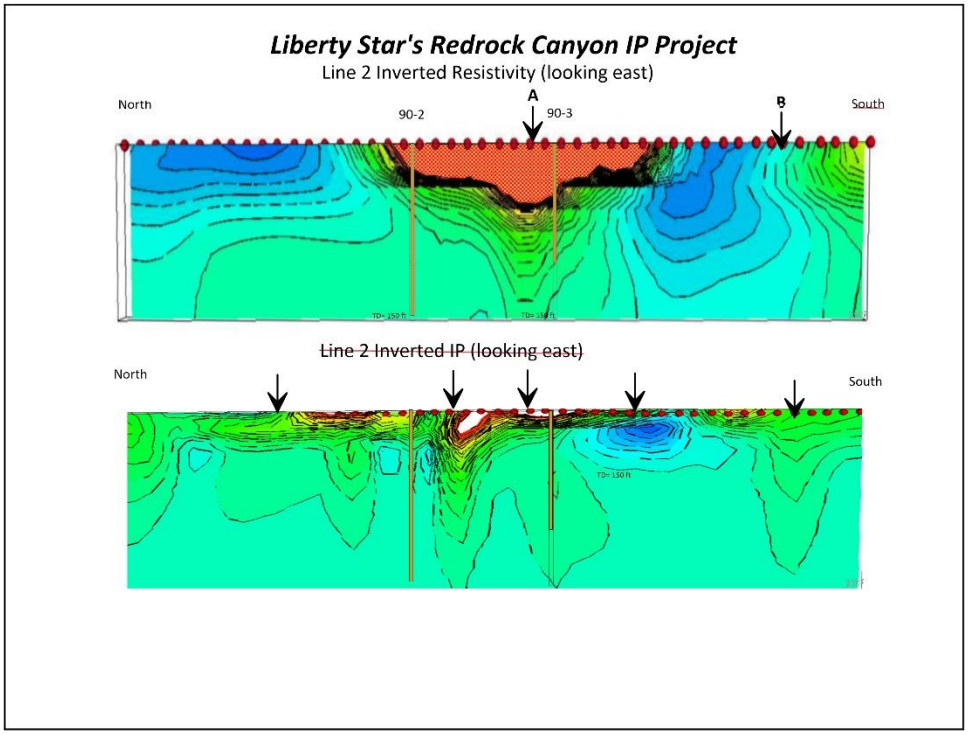

Figure A18: Line 2 inverted sections, looking east.

There are more veins indicated in the raw IP data than are clearly represented in the inverted data but the agreement is mixed. The feeder structure (feature A) is lacking but other features are suggested in the IP section.

Line 3 Inverted Sections

Line 3 resistivity, as with Line 2, shows a correlation with the feeder structure (feature A) but is offset to the south and is still quite broad. Nevertheless, it presents a weak downward trend as desired but the emphasis is much more in the horizontal. The vein at the south end of the line (feature B) is not represented. Vein C at the north end has no expressions in the resistivity but is nicely isolated in the IP data. Otherwise, the northern area is of lower resistivity and corresponds nicely with the raw data.

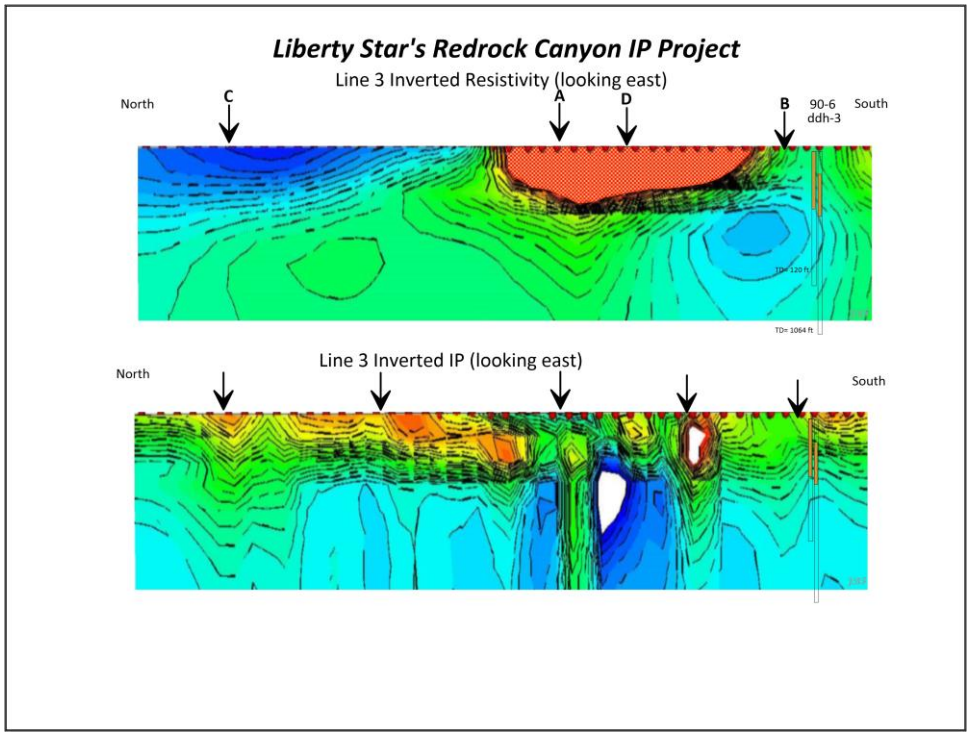

Figure A19: Line 3 inverted sections, looking east.

Line 3 inverted IP data is surprisingly complex, but then, so is the Line 3 raw data section. There are some arguably very good correlations between the two with the only questionable association being that of feature A, the feeder structure. Ideally, it should show up as a higher polarizable feature, compared to the rest of the line, but instead, it displays a neutral or lower response.

Line 4 Inverted Sections

Line 4 resistivity, as previously mentioned, is interpreted as a transitional area for the feeder structure. The high resistivity response is much broader than seen on Lines 1 through 3. In the raw data it was proposed that the feeder structure occurs between stations 390 to 400. It is indicated by "A?". A secondary vein structure is immediately north of "A?" and is unlabeled. It is interesting to note how different the responses are in the inverted data. The most unusual response is noted at depth beneath the north end of the line. The raw data do not support a deep resistive layer but the inverted data show a strongly resistive layer at depth.

The IP data for Line 4 show a quite different response character to that of the resistivity in that there is a much stronger tendency towards vertical features. There is a mix of correlated features and features without correlation.

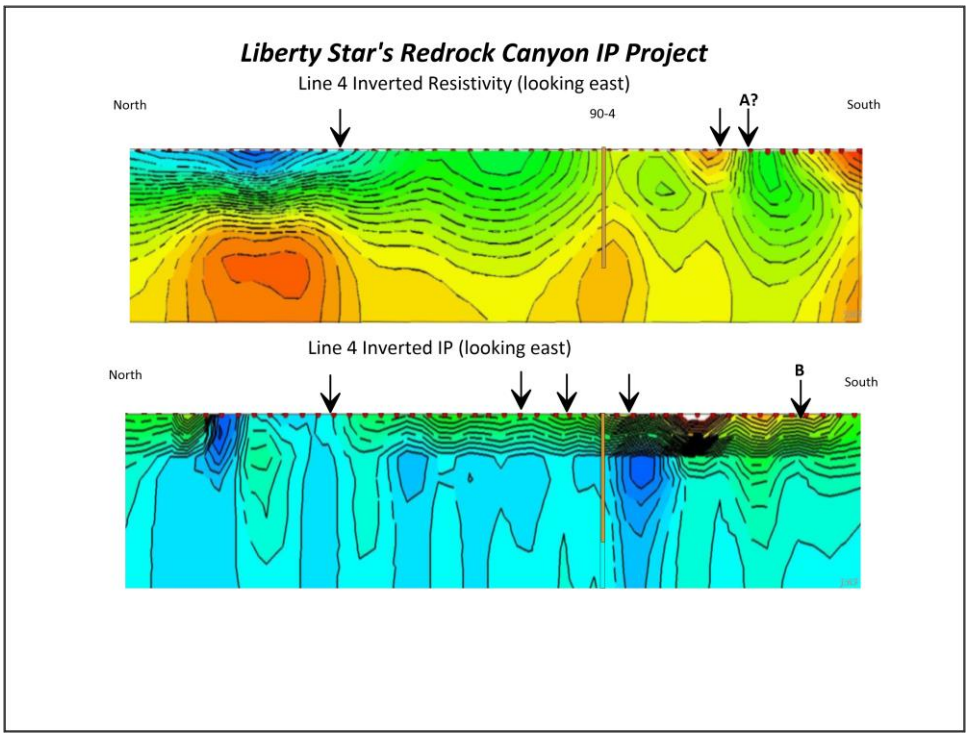

Figure A20: Line 4 inverted sections, looking east.

Line 5 Inverted Sections

The Line 5 inverted resistivity shows a contrasting scenario compared to the raw data. The singular vein-like response at the south end of the line in the raw data is hardly discernible in the inverted data. There is a strong, low resistivity feature at depth approximately between stations 300 to 400 that has no counterpart in the raw data. The remainder of the line to the north appears underlain by a resistive layer. It is difficult to reconcile the strong differences between the inverted and raw data.

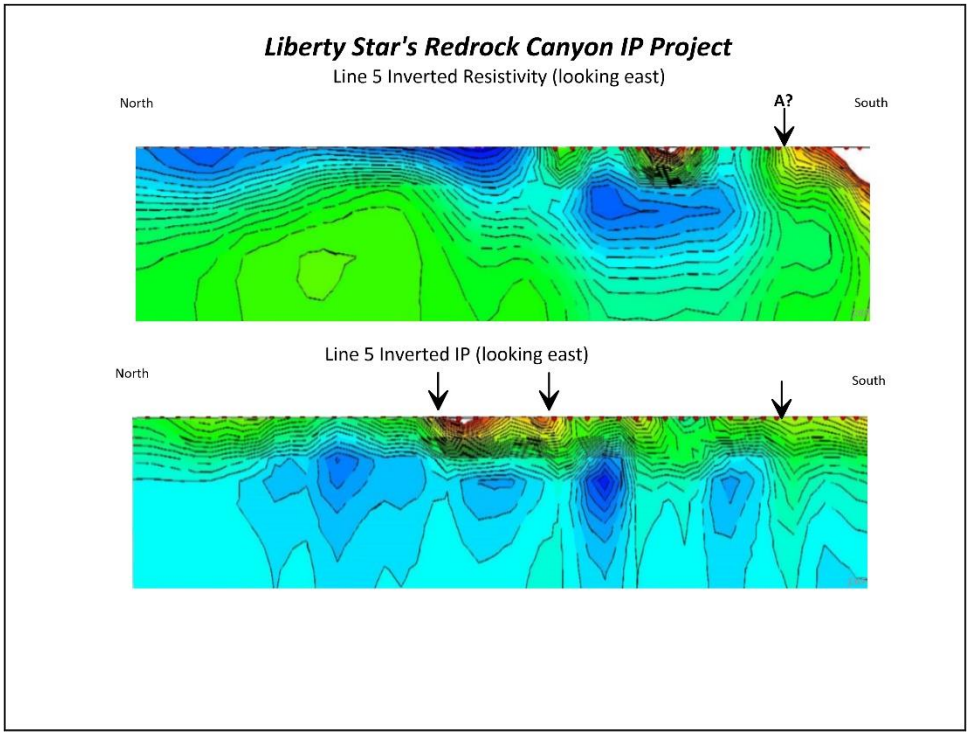

Figure A21: Line 5 inverted sections, looking east.

The inverted IP data show vein-like response beneath the marked areas in good correlation with the raw data. In fact there appears to be a stronger tendency towards vertical features in the inverted IP data than in the raw data. However, instead of the highest IP response occurring at depth as in the raw data the highest inverted IP response is at surface.